



# 1 Long-term patterns of peat accumulation and organic matter 2 decomposition in Costa Rican peatlands

3 Hannah Mitchell<sup>1</sup>, Julie Loisel<sup>1</sup>, Jacklyn Rivera Wong<sup>2</sup>, Alessandra C. Leri<sup>3</sup>, Mia Allison<sup>1</sup>

4 <sup>1</sup>Department of Geography, University of Nevada, Reno, Reno, NV, 89557, USA

5 <sup>2</sup>Ministerio de Ambiente y Energía, Gobierno de Costa Rica, San José, Costa Rica

6 <sup>3</sup>Department of Natural Sciences, Marymount Manhattan College, 221 E 71st St., New York, NY 10021, USA

7 *Correspondence to:* Julie Loisel (jloisel@unr.edu)

8

9 **Abstract.** Tropical peatlands, compared to their boreal counterparts, are vastly understudied despite these ecosystems acting as a  
10 significant terrestrial carbon sink, sequestering 100-300 gigatons of carbon. In particular, the low number of field-based studies  
11 from Latin America and the Caribbean limits our knowledge of these important wetland ecosystems: across the tropical  
12 Panamerican region, peatland location, soil characteristics, inception ages, and carbon accumulation histories remain largely  
13 unknown. These datasets are needed to inform a mechanistic understanding of why peat develops in certain areas but not in others,  
14 both in terms of peat initiation conditions as well as the factors that enable peat to subsist over centuries and millennia. Here we  
15 present extensive, high-resolution laboratory datasets from 11 peat cores from four peatland types from Costa Rica (high-elevation,  
16 riverine, coastal palm swamp, and mangrove). A multi-proxy palaeoecological approach was employed to shed light on the  
17 successional pathways and past conditions that have allowed these peatlands to form, as well as to provide a first estimate of their  
18 carbon stock. The core characterization includes radiocarbon dating, loss-on-ignition, carbon and nitrogen content, and plant  
19 macrofossils. Fourier transform infrared spectroscopy (FTIR) was also used to assess changes in organic matter quality across sites  
20 and over time, ultimately to clarify the role of recalcitrant material in tropical peat accumulation. Overall, this research provides a  
21 basis for understanding long-term carbon accumulation within Caribbean tropical peatlands and is critical to advancing knowledge  
22 of the structure of tropical peatland systems.

23

## 24 1 Introduction

25 Tropical peatlands are estimated to occupy around 14%, and potentially up to 30%, of the global peatland area (Gumbrecht et al.,  
26 2017; UNEP, 2022; Xu et al., 2018). Carbon stock estimates for tropical peatlands similarly vary by a factor of about two, from  
27 ~120-130 gigatonnes (Dargie et al., 2017; Leifeld and Menichetti, 2018) to 288 gigatonnes (Ribeiro et al., 2021). The reason for  
28 these large ranges is multifold and mainly attributable to the scarcity of field-based datasets pertaining to (1) peatland distribution  
29 / surface area, (2) peat depth, and (3) peat carbon density (Gumbrecht et al., 2017; Melton et al., 2022; Page et al., 2011). At times,  
30 the tropical peatland carbon pool has been estimated on the basis of peat carbon density datasets from extra-tropical regions (Yu  
31 et al., 2010), adding unquantifiable uncertainties. Similarly, averaged bulk density and carbon concentration values from Southeast  
32 Asian peatlands have been extrapolated to the Panamerican region due to a lack of data (Page et al., 2011). These data and  
33 knowledge gaps undermine our ability to quantify the tropical peatland soil carbon pool and assess the past, present, and future  
34 roles of these ecosystems in the global carbon cycle.

35



36 In the tropics, the existence of peat has often been referred to as ‘surprising’. This idea stems from the notion that tropical terrestrial  
37 ecosystems tend to be characterized by rapid rates of microbial decomposition due to consistently hot and humid conditions (Knorr  
38 et al., 2005; Meentemeyer, 1978). The accumulation of peat in the tropics therefore requires special conditions that either dampen  
39 the intensified decomposition process near the soil surface and/or a carbon-soil storing mechanism that bypasses the aerobic decay  
40 zone. Previous studies have proposed the following conditions and mechanisms, which are not mutually exclusive: (1) peat soils  
41 must be flooded (or waterlogged all the way up to the near surface) for long enough throughout the year to induce anoxia, which  
42 limits organic matter decay and allows for peat buildup (Chimner and Ewel, 2005; Gillman et al., 2015); (2) plant litter inputs to  
43 the peat must be very high to maintain a positive balance between litter production and peat decomposition; (3) the peat litter is  
44 composed of recalcitrant compounds and/or abundant stems, branches, and wood, all of which inhibit decomposition (Couwenberg  
45 et al., 2010; Dommain et al., 2015; Hodgkins et al., 2018; Hoyos-Santillan et al., 2015; Phillips et al., 1997; Verbeke et al., 2022;  
46 Wright et al., 2013); and (4) root biomass inputs (down into the constantly anoxic zone) circumvent the intensive near-surface peat  
47 decomposition processes and lead to peat buildup (Chimner & Ewel, 2005).

48

49 The bulk of the literature on tropical peatland carbon storage dynamics stems from Southeast Asia (Cobb et al., 2024; Dadap et  
50 al., 2022; Dommain et al., 2015; Hergoualc’h and Verchot, 2011; Hoyt et al., 2020; Ruwaimana et al., 2020; Sasmito et al., 2025)  
51 and, to a lesser extent, the Congo Basin (Dargie et al., 2017; Crezee et al., 2022; Garcin et al., 2022; Young et al., 2023). In the  
52 lowlands of Latin America and the Caribbean (LAC), a region that may encompass the largest tropical peatland complexes in the  
53 world (Gumbrecht et al., 2017), regional knowledge on peatland distribution, extent, and dynamics remains sparse. Across this  
54 region, the most extensive work has been performed in Western and Central Amazonia (Lähteenoja et al., 2009, 2012, 2013;  
55 Lähteenoja and Page, 2011; Draper et al., 2014; Dargie et al., 2024; Winton et al., 2025; Roucoux et al., 2013; Lawson et al., 2014,  
56 2026; Hastie et al., 2022), leaving Central America and the Caribbean particularly understudied. One exception is the Changuinola  
57 peat deposit in Bocas del Toro, Panama, where detailed paleoecological information reveals the historical peatland developmental  
58 pathways (Cohen et al., 1989; Phillips, 1995; Phillips and Bustin, 1996; Phillips et al., 1997; Swindles et al., 2024). A few studies  
59 have also looked at carbon and water dynamics in the Changuinola peatlands (Baird et al., 2017; Girkin et al., 2025; Hedgpeth et  
60 al., 2025; Hoyos-Santillan et al., 2016; Sjögersten et al., 2020). But beyond Changuinola, there is little knowledge on where peat  
61 is found, how deep, old, and carbon-rich it might be, and what factors control long-term peat accumulation processes (Rabel and  
62 Loisel, 2024).

63

64 In this study, we present high-resolution, multi-proxy analyses from a series of peat cores that were collected across 9 sites that  
65 span four distinct hydroecoclimatic and geomorphic settings. The main goal of the study is to characterize peat accumulation  
66 dynamics across these diverse sites and decipher spatial and temporal differences across those peatlands, if any. First, we provide  
67 the paleoecological history from four of our study sites to document changes in the major peat-forming plant macrofossil types  
68 and humification to identify successional pathways. We also discuss the differences that were found across our sites. Second, we  
69 present peat basal ages for our 9 study sites to assess the timing of peat inception in Costa Rica. Third, we provide a suite of  
70 geochemical measurements (organic matter content, dry bulk density, carbon and nitrogen content, C/N ratio) that can be used to  
71 estimate carbon storage. Lastly, through the use of infrared spectroscopy, we endeavor to improve our understanding of the peat  
72 formation process itself. By correlating our plant macrofossil and von Post humification analyses with Fourier-Transform infrared  
73 spectroscopy (FTIR) data, we identify shifts in organic matter quality that coincide with successional changes and/or humification.



74 For instance, the accumulation of recalcitrant compounds (e.g., aromatics) is expected in the deeper portions of the peat, alongside  
75 high levels of humification. An alternative scenario combines high root abundance with carbohydrate compounds at depth, which  
76 could indicate that peat buildup relies, at least in part, on root accumulation that bypasses the oxic zone. Overall, the findings of  
77 this study shed light on biogeochemical processes that underpin the formation, development, and resilience of tropical peatland  
78 ecosystems, thus providing knowledge to scientists, landowners, managers, and policymakers.

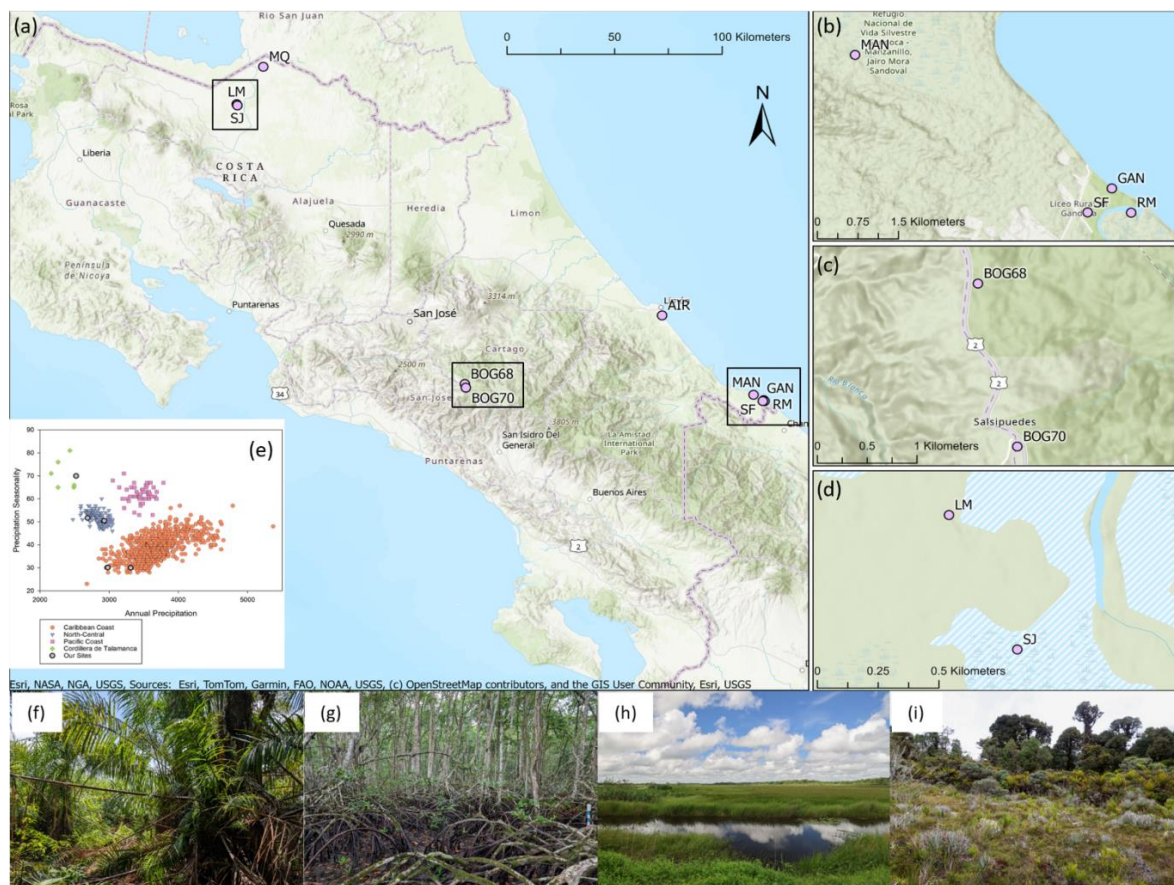
## 79 2 Methods

### 80 2.1 Study area

81 While Costa Rica is rarely mentioned as a peat-rich country, a recent probabilistic map suggests that it may harbor 1456 km<sup>2</sup>,  
82 equivalent to 3% of its land area (Rabel et al. 2025; Fig. 1). With that said, it is important to note that Costa Rica does not yet  
83 possess an official peatland inventory. In July and August 2023, our team traveled across Costa Rica and visited over 15 sites  
84 (Loisel et al., 2024) that had been identified on the basis of published wetland and vegetation maps as well as few existing peat  
85 depth point data (SINAC, 2018; Villegas-Mejía, 2018). We corroborated those data with global-scale peatland probability maps  
86 (Gumbrecht et al., 2017; Melton et al., 2022) and a preliminary map that was produced by Peters and Tegetmeyer (2019). In most  
87 places that were visited, we found peaty soils (i.e., organic-rich soil layers in excess of 30 cm in thickness, *sensu* Lourenco et al.,  
88 2023). Our site selection was ultimately based on site accessibility as well as regional representativity, such that we made sure to  
89 sample the following peatland types: coastal peat swamps, mangroves, riverine complexes, and montane peatbogs (Jiménez, 2016).

90  
91 Costa Rican peatlands are found under a broad range of mean annual precipitation and precipitation seasonality (Rabel et al., 2025;  
92 Fig. 1), and different peatland types are delineated within this climate space. As such, the main peatland types mentioned above  
93 are also distinct in terms of their climatology: the Caribbean coastal sites (palm swamps and mangroves) receive high annual  
94 precipitation amounts with low precipitation seasonality (and annual precipitation increasing along a north-to-south latitudinal  
95 gradient along the coast), whereas the (inland) riverine sites are intermediate in both annual precipitation and its seasonality, which  
96 contrast with the montane sites that are characterized by lower annual precipitation with higher precipitation seasonality.

97



98

99

100 **Figure 1: Locations and photos of sites from this study. (a) The country-wide Costa Rica map, (b) Inset map of the MAN, RM, and GAN**

101 **sites, (c) Inset map of the BOG70 and BOG68 sites, and (d) Inset map of the LM and SJ sites. (e) Climate envelope for Costa Rican**

102 **peatlands, adapted from Rabel et al., 2025. Each circle represents a pixel that has been classified as peat. Photos of the sites include: (f)**

103 **The coastal palm swamp “Gandoca”, (g) The “Red Mangrove” site, (h) The riverine wetland complex “Medio Queso”, and (i) the high-**

104 **elevation “Bog 70” peatland. Photo credits: Hannah Mitchell and Patrick Campbell. Source for panels a-d: Esri, TomTom, FAO, USGS | Powered by Esri.**

105 **2.2 Study sites**

106 The sections below describe the four main peatland types that were sampled and provide information for each coring site. Table 1

107 offers a summary of the most relevant information.

108

Peatland region	Site code	Site name	Latitude	Longitude	Elevation (m)	Peat depth (cm)	Full cores (n)	Bottom cores (n)
High elevation	BOG70	Bog 70	9.64768	-83.84597	2755.5	100	1	0
	BOG68	Bog 68	9.66292	-83.84952	2663.2	80	0	1



Palm swamp	GAN	Gandoca	9.59253	-82.60241	10.8	130	1	1
	AIR	Airport	9.96024	-83.02612	6.1	140	0	1
	MAN	Manzanillo	9.61640	-82.64393	14.3	239	0	1
Mangrove	RM	Red Mangrove	9.58899	-82.59794	14.4	187	1	0
Riverine	MQ	Medio Queso Laguna Martin	11.03382	-84.68874	32.2	230	1	1
	LM	San Jeronimo	10.86676	-84.80004	35.7	96	0	1
	SJ		10.86676	-84.80004	35.7	208	0	1

109

110 **Table 1: Summary information for the Costa Rican peatland study sites.**

111

112 (1) Coastal palm swamps (n = 3) Those sites are located along the southern Caribbean coast of Costa Rica, between the towns of  
 113 Gandoca and Limón. All three sites are dominated by palm swamp species *Raphia taedigera* and harbor other plants, shrubs, and  
 114 tree species, such as *Camposperma panamensis* (Cortés, 1998; Peters and Tegetmeyer, 2019). These coastal sites have developed  
 115 in back-barrier topographic lows, in close proximity to the coastline (Fig. 1). The Gandoca site (GAN) is located in the southern  
 116 part of the country, close to the Panama border; two peat cores were collected along a 1km-long transect that crosses the site (GAN-  
 117 4; GAN-SF). The Manzanillo site (MAN) is located approximately 10 km north of GAN and it is part of the Gandoca-Manzanillo  
 118 Wildlife Refuge and Ramsar site #783 (Ramsar, 2026). Lastly, the Airport site (AIR) is located just south of Limón, in Moín.  
 119 Those three sites were either accessed by boat (via canals) or on foot. To our knowledge, these ecosystems remain unstudied, with  
 120 the exception of prospective work in the 1980s and 1990s that was aimed at assessing the potential economic development of these  
 121 peat deposits as fuel resources (Obando et al., 1995; Thayer et al., 1995).

122

123 (2) Mangroves (n = 1) The Red Mangrove site (RM) is located a few meters away from the Gandoca site (Fig. 1). These two  
 124 ecosystems are separated by Laguna Gandoca, a meandering stream that reaches the Atlantic Ocean. The northern side of the  
 125 stream supports peat-forming *Raphia taedigera* palm swamps, which are probably also aided by the back-barrier geomorphology  
 126 that limits saltwater intrusion, whereas the southern shore is instead characterized by brackish water, tides, and *Rhizophora mangle*  
 127 communities. As only 1% of Costa Rica's mangrove forests are located along the Caribbean coast, our RM site presents a rare  
 128 opportunity to study one of the largest (and preserved) mangrove stands along the Caribbean coast (Álvarez-Sánchez and Piedra-  
 129 Castro, 2020; Cortés, 1998, 2016). There are local studies on the floristic composition of those mangroves (Álvarez-Sánchez and  
 130 Piedra-Castro, 2020) as well as the physico-chemical characterization of the Gandoca Lagoon (Coll et al., 2004), but otherwise  
 131 there is little information on mangrove soil properties from this region with the exception of a study pointing to high soil organic  
 132 matter content in the Gandoca mangroves (Rovai et al., 2018).

133

134 (3) Riverine sites (n = 3) Those sites are located in the north-central portion of Costa Rica, near the Nicaraguan border (Fig. 1).  
 135 The riverine sites all constitute peatland/wetland complexes that experience relatively large water table level fluctuations on an  
 136 annual basis, with surface flooding that can reach 2 m during the wet season (Moreno-Casasola and Warner, 2009; Pérez-Castillo



137 et al., 2024). The ‘Medio Queso’ site (MQ) is located approximately 1 km away from the town of Los Chiles and is found within  
138 the watershed of the Rio Medio Queso. This wetland complex is used for pasture and it is frequently burned to maintain land  
139 clearing (Camacho-Navarro et al., 2017; Pérez-Castillo et al., 2024). A recent study at the site evaluated the impacts of fires on  
140 vegetation and surface peat chemistry (Camacho-Navarro et al., 2017; Pérez-Castillo et al., 2024). The MQ study site is primarily  
141 colonized by rushes (*Eleocharis interstincta*), though many sedge and small bush species are also found (Obando and Malavassi,  
142 1993), along with small ‘islands’ of Cuba palm (*Acoelorrhapha wrightii*). At the time of sampling (August 2023), the wet season  
143 had begun, but we were nevertheless able to walk onto the peatland to retrieve peat cores. Two peat cores (MQ-9; MQ-10) were  
144 collected along a 500 m-long transect that runs from the western edge of the site towards Rio Medio Queso. Our other two riverine  
145 study sites are located within a lagoon complex that is primarily fed by Ríos Frío and Mónico. The lagoon is part of the Caño  
146 Negro Wildlife Refuge and Ramsar site #541 (Ramsar, 2026), which is classified as a mixed-use protected wild area that is home  
147 to local communities who make sustainable use of the ecosystem through subsistence and cultural connections (Jiménez, 2018).  
148 The two study sites (San Jeronimo (SJ) and Laguna Martin (LM) are located within 1 km of one another; the vegetation  
149 communities are dominated by *Eleocharis equisetoides* and *Scleria microcarpa* (Jiménez, 2018). The SJ and LM sites were  
150 accessed by boat and the peat cores were extracted from the boat platform, as the coring sites were flooded by approximately 1m  
151 of water at the time of core collection (August 2023). We did not find any published soil information about Caño Negro.

152

153 (4) Montane peatbogs (n = 2) These sites are located in the Cordillera de Talamanca, Ramsar site #1286 (Ramsar, 2026), in central  
154 Costa Rica. In this high-elevation area (~ 3000 m.a.s.l.), peatlands tend to be very small in size (often < 0.05 km<sup>2</sup>; Rabel et al.  
155 2025). Their existence has been linked to the mountain range’s Late Pleistocene glacial history, with montane peatlands forming  
156 in small, poorly drained depressions following the last deglaciation around 10,000 years ago (Horn, 1990). Today, the area is  
157 considered part of a subalpine paramo ecosystem, itself located within a cloud forest, with a cool and moist climate, and the small  
158 peatland-bearing depressions are prone to seasonal flooding (Jiménez, 2016). The two sites that we sampled, Bog 70 and Bog 68,  
159 were named after the km markers on the side of the road (Rodgers and Horn, 1996). Those sites are dominated by a unique mixture  
160 of peat moss (*Sphagnum* sp.), reindeer lichen (*Cladonia rangiferina*), and tropical plants such as tree ferns (*Blechnum auratum*),  
161 bromeliads (*Puya dasyliroides*), and numerous herbaceous species (see Rodgers and Horn (1996) for details). Sediment cores  
162 have been retrieved from these sites before and used for pollen-based paleoenvironmental reconstructions (Hooghiemstra et al.,  
163 1992; Islebe et al., 1995, 1996), but studies of the peat characteristics themselves were not conducted to our knowledge.

### 164 2.3 Field sampling strategy and approach

165 The work herein stems from an exploratory trip; we opted for visiting a larger number of sites while obtaining fewer data points  
166 for each site. The general approach that was used to sample sites included: (1) trace a transect line from the edge of a potential  
167 peatland towards its center, (2) walk (or boat) along said transects, and (3) probe the soil along the transects to confirm the presence  
168 (or absence) of peat. The length and orientation of those transects varied for each site and mainly depended on site conditions and  
169 time constraints. Peat depth and coordinates were recorded for each probing.

170

171 A ‘full core’ was retrieved from the deepest portion of four peatlands using a 50 cm long, 5 cm diameter Russian-style peat borer.  
172 A full core consists of the entire peat column, from the peatland surface to the peat-to-mineral interface. The multi-proxy analyses  
173 presented in this study were performed on those four cores. In addition to these full cores, several ‘bottom cores’ (n = 7) were



174 collected along the transects from all 9 peatlands (Table 1). Those bottom cores consist of the deepest 50 cm long drive that was  
175 collected at the site and they include the peat-to-mineral interface. Those bottom sediment cores are primarily used to analyze  
176 patterns in peat basal ages along transects, which may help understand the history of peatland expansion across individual basins.  
177 In the field, all freshly collected cores were placed in PVC pipes and wrapped in plastic film and aluminum foil. The samples were  
178 kept at 4° C until laboratory analysis.

#### 179 **2.4 Laboratory sample preparation and analysis**

180 In the laboratory, all peat cores were photographed and sliced into contiguous, 1 cm thick slices, which were then placed into  
181 labeled plastic bags and stored at 4° C. The following sections describe the methodological approach that was followed to prepare  
182 our samples for different proxy analyses. Although not every analysis was conducted at the same resolution (e.g., every 2 cm for  
183 LOI vs. every 8 cm for FTIR), most measurements were made on the same peat slices to allow for direct comparison across  
184 methods (see Table A1 for a list of proxies and analytical resolution).

##### 185 **2.4.1 Peat geochemistry (loss-on-ignition and elemental analysis)**

186 The loss-on-ignition method was followed (Dean, 1974) to determine peat water content, dry bulk density, and organic matter  
187 content. Every 2 cm, a sub-sample (1 cm<sup>3</sup>) was extracted from the peat slice, weighed, and sequentially oven dried to determine  
188 water content and dry bulk density (40° C, 48 h) as well as organic matter content (550° C, 4 h). These measurements were also  
189 used to calculate organic matter (Loisel et al., 2014).

190  
191 For carbon and nitrogen content determinations, 1 cm<sup>3</sup> sub-samples were collected every 8 cm. Samples were oven dried (40°C)  
192 and ground into a fine powder using a Retsch MM 300 Vibration Mill Mixer (Verder Company, Germany). The homogenized  
193 samples were then placed into tin capsules. C and N content were measured using a Costech ECS 4010 Elemental Analyzer  
194 (Costech Analytical Technologies, Inc., Valencia, CA USA). Different sample weights were used on the basis of organic matter  
195 content, with smaller sample weights for organic-rich samples and vice versa. The carbon-to-nitrogen ratio (C/N) is presented as  
196 a mass ratio. The C/N ratio of peat can be used as a proxy for decomposition and humification (Biester et al., 2014; Kuhry and  
197 Vitt, 1996; Malmer and Holm, 1984). Organic carbon density was subsequently calculated for each sample by multiplying the  
198 organic matter density (from LOI data) with the measured C content. Finally, the regression between peat C% and peat OM% is  
199 presented as an estimate for organic carbon content that can be used in future studies that may lack elemental analysis.

##### 200 **2.4.2 Peat organic matter quality (FTIR spectroscopy)**

201 FTIR spectroscopy was used to analyze peat organic matter quality (Artz et al., 2008; Holmgren and Nordén, 1988; Krumins et  
202 al., 2012; Uhelski et al., 2022). FTIR spectroscopy has been shown to be a useful proxy for humification index in a peat column  
203 (Biester et al., 2014; Broder et al., 2012; Tfaily et al., 2014; Upton et al., 2018). Sub-samples (1 cm<sup>3</sup>) were collected every 8 cm  
204 along the four full cores. Samples were oven dried (40° C) and ground into a fine, homogenized powder using a Retsch MM 300  
205 Vibration Mill Mixer. Spectra were acquired on a Thermo Nicolet 380 FTIR spectrometer (Thermo Electron Scientific Instruments  
206 Corporation, Madison, WI USA) by averaging 100 scans at 8 m<sup>-1</sup> resolution over a range of 4000-550 cm<sup>-1</sup>. Samples were placed  
207 directly on an attenuated total reflectance (ATR) crystal, and light force was applied so the samples came into direct contact with  
208 the crystal. ATR correction and atmospheric suppression took place to account for variability in background CO<sub>2</sub> and water vapor.



209 A background scan was collected before every sample. The spectra were then manually baseline-corrected between 4000-3750  
210 and 2600-1800  $\text{cm}^{-1}$ . A custom R script (R Core Team, 2024) was used to determine the peak heights and relative abundances of  
211 carbohydrates, aromatics, acids, and aliphatics in predetermined regions of the spectra (Hodgkins et al., 2018; Fig. A1). The ratios  
212 of carbohydrates/aromatics, carbohydrates/aliphatics, and aromatics/aliphatics were also calculated.

### 213 **2.4.3 Peat composition (plant macrofossils and von Post humification index)**

214 Plant macrofossils were analyzed following standard procedures (Loisel et al., 2009; Mauquoy et al., 2002). Sub-samples (1  $\text{cm}^3$ )  
215 were analyzed every 8 cm (or at higher resolution near stratigraphic boundaries) along each full core. Samples were mixed with  
216 deionized water and suspended in a petri dish, then scanned under a stereomicroscope. The first step involved the visual estimation  
217 of the percentage of mosses, herbaceous, ligneous, mineral, and unidentified plant material (UOM) (Mauquoy et al., 2010). A peat  
218 type category (bryophyte, herbaceous, ligneous) was assigned to each sample on the basis of the plant macrofossil analysis, where  
219 the dominant plant type found in each sample was used to infer the peat type (Loisel et al., 2014). We note that the 'ligneous' peat  
220 type was split into two sub-categories: ligneous-general vs. ligneous-mangrove to better represent our peat material. Lastly, we  
221 specified the presence of 'root material' both herbaceous and ligneous material when possible. We note that this differentiation is  
222 often challenging, given structural similarities between aerial vs. subterranean plant tissue. But in some cases, such as for mangrove  
223 roots, the distinction was safe to make.

224

225 Peat humification was determined at 8cm increments using the von Post humification scale (ASTM, 1987), a simple, widely used  
226 method to estimate the level of peat decomposition by pressing and manipulating a small sample of peat ( $\sim 1 \text{ cm}^3$ ) in one's hands  
227 (Kaila, 1956; Rydin and Jeglum, 2013; Stanek and Silc, 1977).

### 228 **2.4.4 Peat basal ages and chronologies (radiocarbon dates and age-depth models)**

229 Peat inception ages were determined using radiocarbon ( $^{14}\text{C}$ ) dating (Table 2). Along each core, the deepest (and presumably  
230 oldest) peat sample was identified using LOI results (see below). A 30% organic matter threshold was used to identify the peat-to-  
231 mineral boundary along our peat cores (Joosten and Clark, 2002; Lourenco et al., 2023). Given the humic nature of the peat, dated  
232 samples consisted of bulk, root-free samples (63-125  $\mu\text{m}$ ). Samples were wet-sieved using deionized water, oven dried at 40° C,  
233 and packaged in aluminum foil. Additional samples were extracted along the four full cores and similarly prepared for  $^{14}\text{C}$  dating,  
234 to generate peat accumulation histories. Samples were shipped to Lawrence Livermore National Laboratory's Center for  
235 Accelerator Mass Spectrometry (CAMS), where they underwent acid-base-acid (ABA) treatment (Gillespie and Hedges, 1983;  
236 Hedgpeth et al., 2025; Norris et al., 2020). Dates were first individually calibrated to calendar age (cal. yr BP) using the Intcal20  
237 calibration curve (Reimer et al., 2020) in CALIB v8.2 (Stuiver and Reimer, 1993). As for constraining peat chronologies of the  
238 full cores using multiple  $^{14}\text{C}$  ages, a Bayesian age-depth modeling approach was used (package *rbacon*) v.3.5.2 in R (Blaauw and  
239 Christen, 2011).

240

Core name	Sample Depth (cm)	$^{14}\text{C}$ Age (years BP)	Error ( $\pm$ )	Median Age (cal. yr BP)	Error (2 sigma) ( $\pm$ )	Laboratory ID (CAMS)
BOG70	21.5	>Modern*		-59	2	195269



	100.5	8765	35	9759	173	193837
BOG68	80.5	9640	90	10967	248	193857
GAN-4	45.5	220	25	173	77	193839
	90.5	350	25	435	77.5	193838
	130.5	725	25	668	72.5	193836
GAN-SF	170.5	990	35	856	84.5	195199
AIR	140.5	450	25	507	23.5	193832
MAN	223.5	2380	30	2403	161.5	193858
	239.5	2595	25	2740	18	193835
RM	47.5	315	25	389	75	193842
	83.5	220	30	447	57.5	195272
	94.5	495	30	524	23.5	193859
	141.5	895	25	787	86.5	193841
	187.5	1135	25	1021	108.5	193840
MQ-S9	35.5	860	30	802	141.5	195271
	45.5	1785	25	1690	156.5	193845
	59.5	2700	35	2842	147.5	195200
	69.5	3625	35	3998	359	195201
	75.5	4555	35	5233	196	195202
	80.5	5065	30	5806	139	195271
	90.5	5305	25	6082	95.5	193844
	135.5	5885	25	6706	65	193843
	180.5	6855	35	7683	83.5	193860
	MQ-S10	206.5	5690	25	6465	74.5
230.5		7535	30	8361	96	193830
LM	96.5	1840	25	1741	89	193833
SJ	208.5	1085	25	988	64	193831

241 **Table 2: AMS radiocarbon dating results from the new peat cores in Costa Rica. \*The modern age for sample CAMS-195269 returned**  
 242 **a fraction modern of  $1.0520 \pm 0.0041$ .**

## 243 2.5 Statistical Analysis

244 First, an analysis of variance (ANOVA) was used to test the effect of ‘peat type’ on the peat geochemical properties (Loisel et al.  
 245 2014). Second, a correlation matrix was completed in R with the packages *energy*, *corrplot*, *dplyr*, and *ggplot2* to compare the  
 246 relationship between peat proxies (Rizzo and Szekely, 2024; Wei and Simko, 2024; Wickham, 2016; Wickham et al., 2023). To  
 247 account for possible non-linear trends in the data, we opted for a Spearman correlation (Zar, 2005). Third, a Principal Coordinates  
 248 Analysis (PCoA) based on the Bray-Curtis distance was used to capture variations in the peat properties across peat types and sites,  
 249 and over time (Tian et al., 2019). The analysis was performed in R with the *vegan* package (Oksanen et al., 2025). Bray-Curtis  
 250 distances were chosen to understand differences in ecological compositions while also handling the differences in relative  
 251 abundances gathered from the FTIR analysis (Kellerman et al., 2015; Wang et al., 2022). Lastly, PERMANOVA and Distance-  
 252 based redundancy (dbRDA) analyses were performed in conjunction with the PCoA to statistically test differences between sites  
 253 (Anderson, 2001; Legendre and Anderson, 1999; Tian et al., 2019).

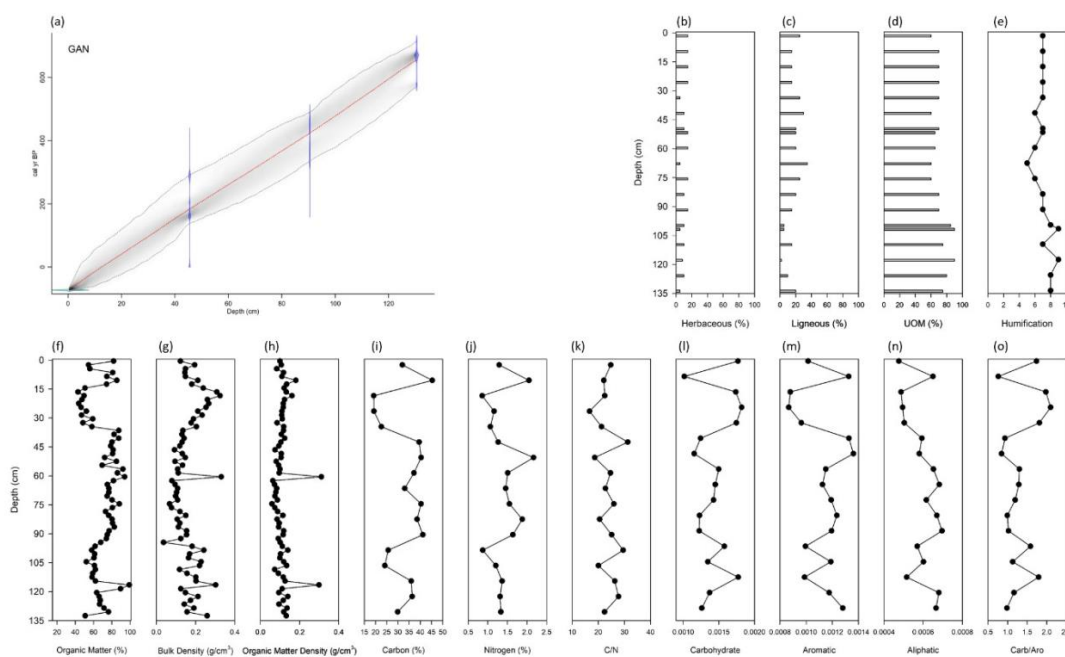


254 **3 Results**

255 **3.1 Peat accumulation histories across four Costa Rican sites**

256 **3.1.1 Coastal palm swamp site (Gandoca - GAN)**

257 The GAN core is characterized by 130 cm of peat that is underlain by fine mineral particles. Peatland initiation began at 668 cal.  
 258 yr BP and the plant macrofossil record, which is dominated by ligneous palm remnants, suggests that a palm swamp community  
 259 has likely occupied this site since peat inception (Fig. 2). The peat humification index was consistently high, with slightly more  
 260 humified peat towards the base of the peat column. The apparent rate of peat accumulation is steady and relatively rapid (0.2  
 261 cm/yr), and the age-depth relationship follows a linear trend. The peat stratigraphy is high in organic matter throughout the profile  
 262 (mean = 70.2%). Expectedly, bulk density tends to be relatively low (mean = 0.164 g/cm<sup>3</sup>), with a sharp peak that corresponds to  
 263 the abovementioned mineral interval. As for peat quality, the GAN core is characterized by low variability in its abundance of  
 264 carbohydrate, aromatic, acid, and aliphatic compounds (Fig. 2 and A2), with the exception of near-surface samples (16 and 24 cm)  
 265 and the mineral transition at the end of the peat (136 cm), where peaks associated with greater amounts of carbohydrates (in  
 266 combination with lower aromatics and aliphatics) were identified.  
 267



268

269 **Figure 2. Accumulation history, macrofossil composition, geochemical, and FTIR results for the coastal palm swamp (GAN) site. (a)**  
 270 **Age-depth model, (b) herbaceous macrofossil composition (%), (c) ligneous macrofossil composition (%), (d) unidentified organic matter**



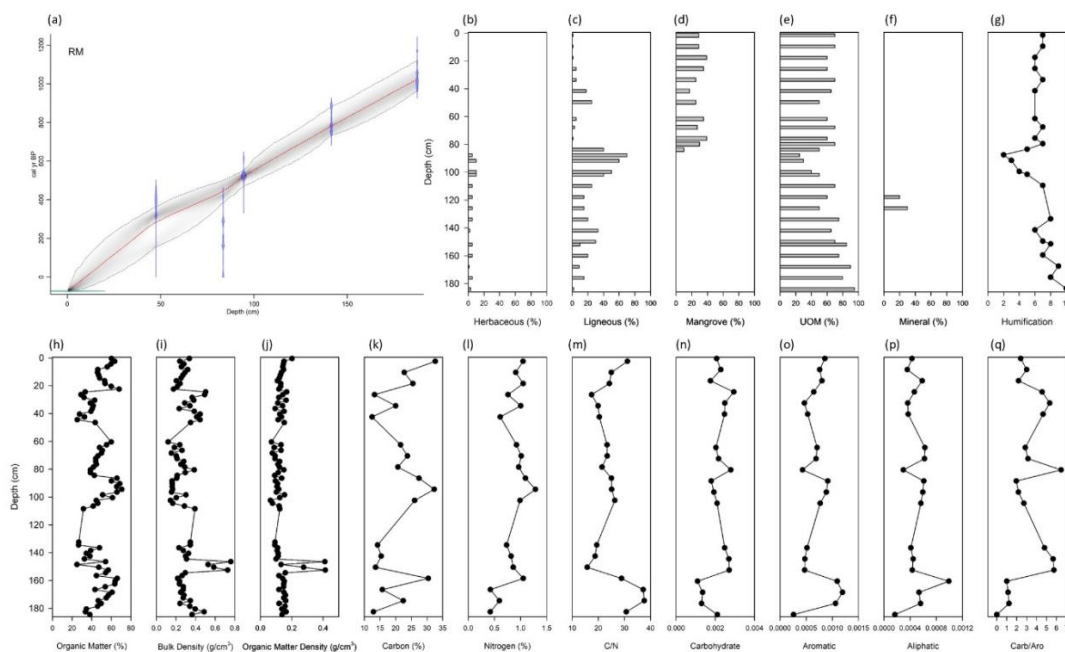
271 (UOM) composition (%), (e) von Post humification, (f) organic matter content (%), (g) bulk density (g/cm<sup>3</sup>), (h) organic matter density  
272 (g/cm<sup>3</sup>), (i) carbon content (%), (j) nitrogen content (%), (k) carbon/nitrogen ratio, (l) carbohydrate abundance, (m) aromatic abundance,  
273 (n) aliphatic abundance, and (o) carbohydrate/aromatic ratio.

### 274 3.1.2 Mangrove site (Red mangrove - RM)

275 The RM core is 187 cm-long and primarily composed of organic-rich material, which is why this site is included in our peat study.  
276 As a point of reference, other mangrove studies in the region have described these ecosystems as mineral-rich, with 5-8% OM  
277 (Rodgers and Horn, 1996). In contrast, our RM site harbors OM% in the order of 25-71%. In addition, the record begins as a palm  
278 swamp that initiated around 1020 cal. yr BP and persisted until 465 cal. yr BP (Fig. 3). The underlying sediment consists of sandy  
279 material, and the stratigraphy is interrupted by one mineral-rich layer around ~740-620 cal. yr BP (110-134 cm). Around 465 cal.  
280 yr BP (83 cm), the stratigraphy abruptly shifts to a dominance of *Rhizophora* plant remnants (mangrove roots). We caution that,  
281 while the shift from palm swamp to mangrove seems to take place at 465 cal. yr BP according to our Bayesian age-depth model,  
282 said model also rejected a <sup>14</sup>C date from a sample that was picked at the ecological transition (83.5cm) but that was deemed ‘too  
283 young’ to fit the rest of the curve (<sup>14</sup>C age: 220 ± 30, which yields a median age of 189 cal. yr BP with a 2-sigma range of 0-310  
284 cal. yr BP; Fig. 3). This age reversal, if representative of the sediment history, would suggest that the ‘mangrove root deposit’ is  
285 in fact much more recent than indicated by the age-depth relationship, possibly as young as a few decades only.

286  
287 The peat humification index is generally mesic to humic, with the exception of relatively undecomposed peat following the  
288 transition from palm swamp to mangrove. The apparent rate of peat/sediment accumulation is steady and relatively rapid (0.2  
289 cm/yr; similar to the nearby GAN core), and the age-depth relationship follows a linear trend - with the caveat of a possible hiatus  
290 at the transition from palm swamp to mangrove (83 cm). The peat stratigraphy is characterized by moderate organic matter content  
291 (mean = 43.83%), the lowest average of all our sites. The RM results are characterized by wide changes between OM-rich (mean  
292 = 47.45%) and mineral-rich (mean = 18.80%) intervals, generally in a reverse relationship with bulk density. Those changes in  
293 organic matter content and bulk density follow a ~ 200-yr cycle (Fig. 3). As for peat quality, the spectroscopic dataset is  
294 characterized by very high peaks within the carbohydrate region of the spectra contrasted by low aromatics, acids, and aliphatics  
295 throughout the core (Fig. 3 and A3). The mineral-rich layer is expressed as flattened spectra (112-128 cm). We note that the  
296 aromatic and aliphatic abundances tend to correlate with %C and %OM, with greater compound abundances corresponding to OM-  
297 and C-rich material. However, some of the carbohydrate peaks correspond to intervals with high bulk density, which is in  
298 opposition with the hypothesized negative relationship between those two proxies. Indeed, the expectation is to see high  
299 carbohydrates correlating with low bulk density, both representing a low degree of decomposition. We offer an explanation of this  
300 incongruent result in sect. 3.1.3 and 3.2.1.

301



302

303 **Figure 3. Accumulation history, macrofossil composition, geochemical, and FTIR results for the mangrove (RM) site. (a) Age-depth**  
 304 **model, (b) herbaceous macrofossil composition (%), (c) ligneous macrofossil composition(%), (d) ligneous mangrove macrofossil**  
 305 **composition (%), (e) unidentified organic matter (UOM) composition (%), (f) mineral composition (%), (g) von Post humification, (h)**  
 306 **organic matter content (%), (i) bulk density (g/cm<sup>3</sup>), (j) organic matter density (g/cm<sup>3</sup>), (k) carbon content (%), (l) nitrogen content (%),**  
 307 **(m) carbon/nitrogen ratio, (n) carbohydrate abundance, (o) aromatic abundance, (p) aliphatic abundance, and (q)**  
 308 **carbohydrate/aromatic ratio.**

### 309 3.1.3 Riverine site (Medio Queso - MQ)

310 The MQ core presents 180 cm of peat material with an inception age of 7683 cal. yr BP. Initially, the site was likely a palm swamp  
 311 (Fig. 4), as shown by the presence of ligneous palm fragments akin to those found at our coastal (GAN) and mangrove (RM) sites.  
 312 The palm swamp ecosystem persisted for at least two millennia (until ~ 5500 cal. yr BP), but perhaps for a longer time interval. A  
 313 hiatus from ~ 5500 to ~ 2500 cal. yr BP (75-55 cm) challenges our ability to determine the timing of the transition into the modern-  
 314 day herbaceous peatland. The apparent long-term rate of peat accumulation for the palm swamp (7683-5500 cal. yr BP) was 0.05  
 315 cm/yr, which is an order of magnitude slower than our observations at GAN and RM. The peat swamp portion of the profile is  
 316 characterized by relatively high OM% (> 50%) and low BD (< 0.3 g/cm<sup>3</sup>), with the exception of two layers with ~ 30% OM and  
 317 densities of ~0.5 g/cm<sup>3</sup>. Those two layers are also associated with very high peaks within the carbohydrate region, which we posit  
 318 are overprinted by silicated minerals (Fig. A4). Indeed, the MQ core exhibits a split peak in the carbohydrate region of the spectra,  
 319 most likely attributed to both organic matter carbohydrates (1030 cm<sup>-1</sup>) and silicate minerals (1005 cm<sup>-1</sup>) (Reig et al., 2002). This  
 320 interpretation is corroborated by the presence of bands at 912, 3620, 3695 cm<sup>-1</sup> that are likely linked to the presence of silicates

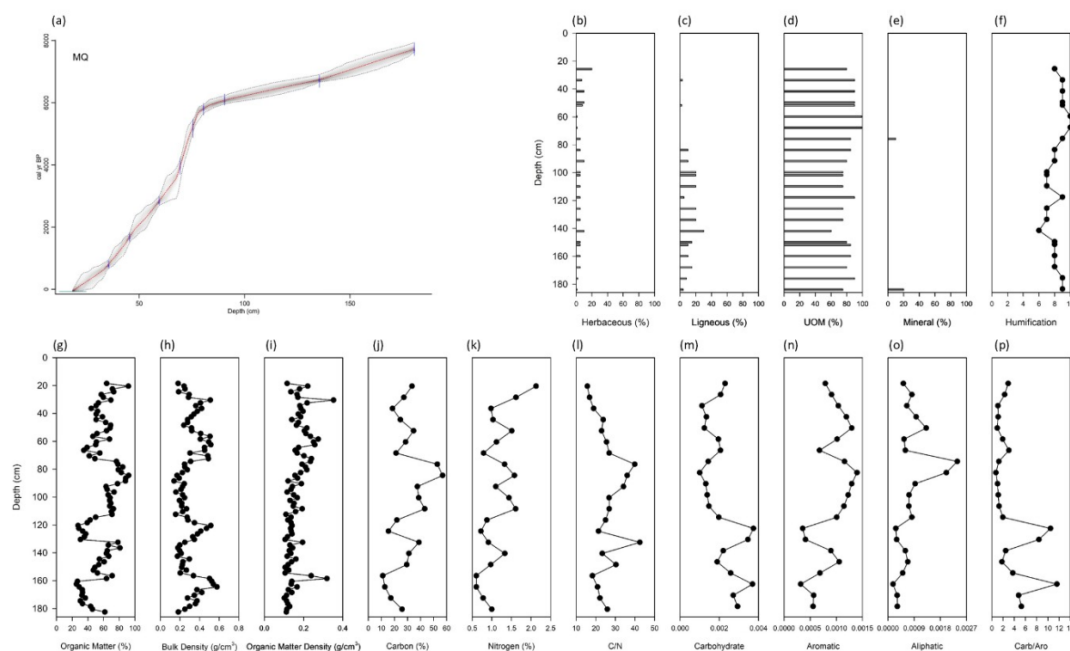


321 and kaolinite clays (Müller et al., 2014; Seaton et al., 2024; Sengyang et al., 2015). Repeated flooding may have increased clay  
 322 content, confounding the carbohydrate signal, thereby also explaining why our high carbohydrate abundances are synchronous  
 323 with high bulk density values, which is also a phenomenon that we observed at our mangrove site (RM; see sect. 3.1.2).

324

325 There is then a long-time interval (from 5500 to ~ 2500 cal. yr BP; from 75 to 55 cm) during which the record may have been  
 326 altered, with a two-fold slowdown in apparent rate of peat accumulation (0.007 cm/yr). This interval coincides with high bulk  
 327 density values ( $> 0.4 \text{ g/cm}^3$ ), humic peat (10 on the von Post scale), and peaks in aliphatics that suggest the presence of herbaceous  
 328 peat. Our field notes also indicate the presence of thin mineral layers throughout this part of the profile. The uppermost peat section  
 329 (top 55 cm) corresponds to the past 2500 years and is composed of herbaceous material with an averaged apparent rate of peat  
 330 accumulation of 0.02 cm/yr. This herbaceous section is characterized by noticeably lower C/N values and the presence of  
 331 herbaceous plant remnants (up to 20%). We note that the uppermost section of the record was compressed during the coring process  
 332 due to the presence of surface water (0-18cm), making it difficult to assess changes in peat properties in the near-surface samples.  
 333 Nevertheless, OM% is highest in the uppermost peat layers (60-95%) and corresponds to low bulk density values ( $< 0.2 \text{ g/cm}^3$ ),  
 334 despite the peat being already very humified near the top of the core (von Post = 8).

335



336

337 **Figure 4.** Accumulation history, macrofossil composition, geochemical, and FTIR results for the riverine (MQ) site. (a) Age-depth model,  
 338 (b) herbaceous macrofossil composition (%), (c) ligneous macrofossil composition (%), (d) unidentified organic matter (UOM)  
 339 composition (%), (e) mineral composition (%), (f) von Post humification, (g) organic matter content (%), (h) bulk density ( $\text{g/cm}^3$ ), (i)

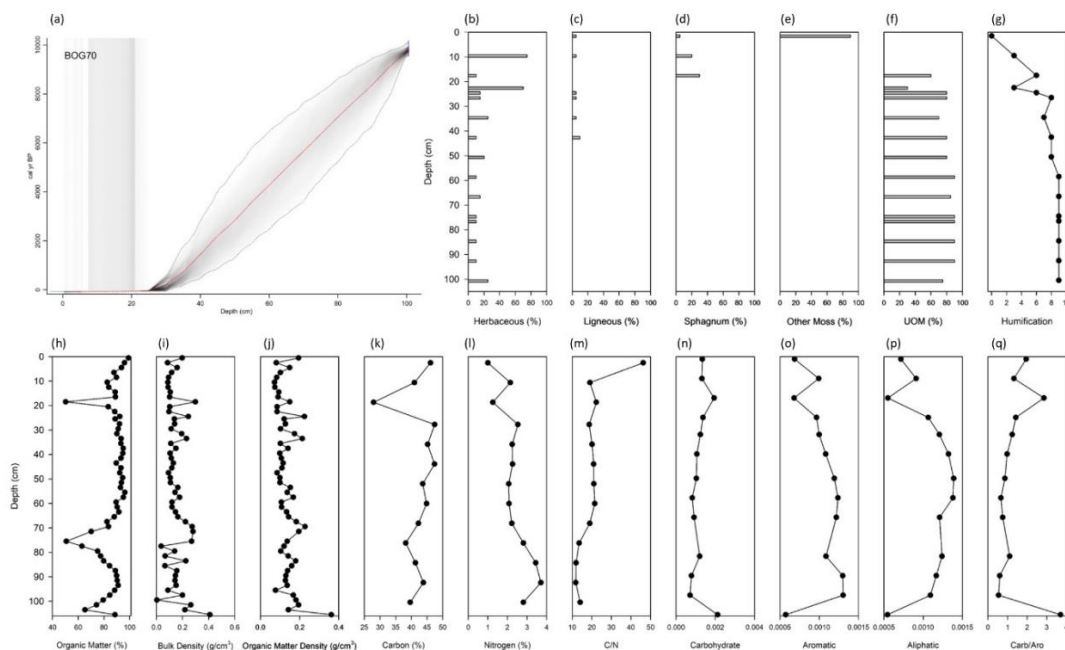


340 organic matter density ( $\text{g}/\text{cm}^3$ ), (j) carbon content (%), (k) nitrogen content (%), (l) carbon/nitrogen ratio, (m) carbohydrate abundance,  
341 (n) aromatic abundance, (o) aliphatic abundance, and (p) carbohydrate/aromatic ratio.

#### 342 3.1.4 Montane site (BOG70)

343 The BOG70 core is our shortest but longest record, at 100 cm and with an initiation age of 9759 cal. yr BP. The ecosystem appears  
344 to have started as a herbaceous-dominated peatland (Fig. 5), atop clayey sediment, though the peat is highly humified, which limits  
345 the use of plant macrofossil analysis. Ligneous fragments were found starting around 1823 cal. yr BP (42 cm). *Sphagnum* and  
346 *Amblystegiaceae* remnants appear in the record at -65 cal. yr BP (18.5 cm) and form the modern-day moss carpet. The apparent  
347 long-term rate of peat accumulation was the slowest of all 4 study sites at 0.01 cm/yr, which is 15-20 times lower than the coastal  
348 palm sites. Peat humification is high along the entire record though it trends towards lower humification towards the top of the  
349 profile. Organic matter content is high throughout the majority of the core (mean = 86.25%); this montane site in fact presents the  
350 highest organic matter content of all 4 study sites. Those results are corroborated by a prior study that reported high organic matter  
351 content (60-96%) for these montane sites (Rodgers and Horn, 1996). The FTIR data show that the record is characterized by low  
352 carbohydrates relative to aromatic and aliphatic components (Fig. 5 and A5). Notably, high aliphatic abundance appears  
353 contemporaneous to the herbaceous peat. There is also a unique signature at the core surface, where the two aliphatic C-H bands  
354 are less resolved than in all the other samples (Fig. A5, top sample). This feature is a hallmark of fresh *Sphagnum* (Heller et al.,  
355 2015). At the base of the peat column (105 cm), an increase in clay content is inferred from spectral features at 3620 and 3695  $\text{cm}^{-1}$ .  
356 <sup>1</sup>.

357



358

359 **Figure 5. Accumulation history, macrofossil composition, geochemical, and FTIR results for the montane (BOG70) site. (a) Age-depth**  
 360 **model, (b) herbaceous macrofossil composition (%), (c) ligneous macrofossil composition (%), (d) *Sphagnum* macrofossil composition**  
 361 **(%), (e) other (non-*Sphagnum*) moss macrofossil composition(%), (f) unidentified organic matter (UOM) composition(%), (g) von Post**  
 362 **humification, (h) organic matter content (%), (i) bulk density (g/cm<sup>3</sup>), (j) organic matter density (g/cm<sup>3</sup>), (k) carbon content (%), (l)**  
 363 **nitrogen content (%), (m) carbon/nitrogen ratio, (n) carbohydrate abundance, (o) aromatic abundance, (p) aliphatic abundance, and (q)**  
 364 **carbohydrate/aromatic ratio.**

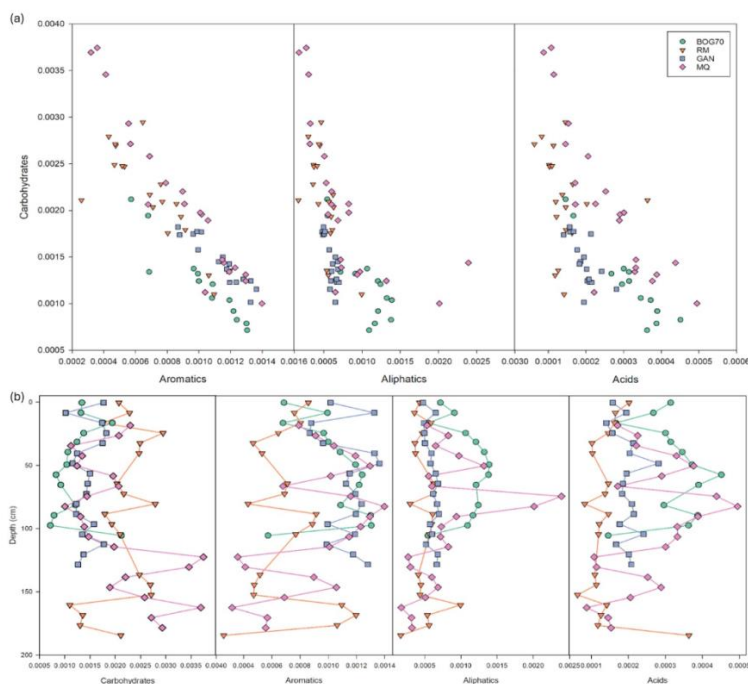
### 365 3.2 Spatiotemporal patterns in peat properties

#### 366 3.2.1 Peat organic matter quality (FTIR data)

367 Correlations between functional groups were found across all sites (Fig. 6 and A6), with carbohydrates negatively correlated with  
 368 aromatics (Spearman = -0.881,  $p < 0.0001$ ), aliphatics (Spearman = -0.794,  $p < 0.0001$ ), and acids (Spearman = -0.679,  $p < 0.0001$ ).  
 369 We also note that aromatics, and especially aliphatics, correspond with %C and %OM, confirming these spectral features as proxies  
 370 for stable organics (Fig. A6). All those associations are stronger at the site level (Fig. 6), though downcore trends are complex. For  
 371 instance, the coastal swamp site (GAN) and the montane site (BOG70) both show progressive decreases in carbohydrates with  
 372 depth inverse to the increases in aromatic and aliphatic abundances. This pattern is expected, as carbohydrates represent  
 373 comparatively labile organic matter, whereas aromatic and aliphatic moieties tend to show greater long-term stability and are  
 374 thought to ‘accumulate’ in older, more refractory peat (Leri et al., 2025; Verbeke et al., 2022). We note that aliphatic abundances  
 375 are greater at the montane, herbaceous-dominated site (BOG70) than in the lowland, ligneous-dominated swamp (GAN). As for

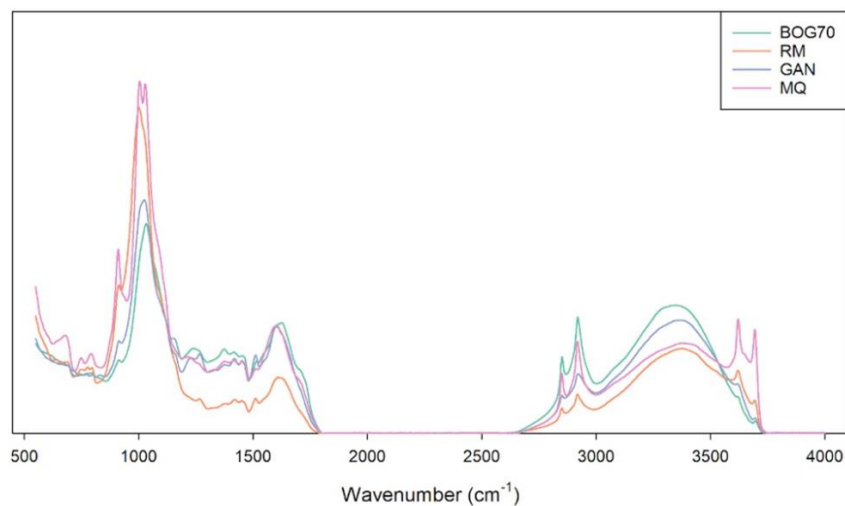


376 the riverine (MQ) and mangrove (RM) sites, large variations along the core do not follow the expected increase in recalcitrant  
 377 fractions with depth.  
 378



379  
 380 **Figure 6. FTIR data from our four Costa Rican peatlands. (a) the relative abundances of carbohydrates are plotted against aromatics,**  
 381 **aliphatics, and acids, (b) changes in carbohydrates, aromatics, aliphatics, and acids are shown as time series (i.e., along peat core depth).**

382 Average spectra from all of the depths in each core were compared (Fig. 7) in an attempt to detect site-specific signatures. The  
 383 presence of distinct dual aliphatic C-H features ( $2850$  and  $2920\text{ cm}^{-1}$ ) across all sites indicate high organic matter content and the  
 384 presence of peat (Martínez Cortizas et al., 2021). As mentioned above, the coastal peat swamp (GAN) and the montane site  
 385 (BOG70) exhibit similarities in terms of their averaged carbohydrate and aromatic content, though the herbaceous site (BOG70)  
 386 is characterized by greater aliphatic content. Conversely, the mangrove (RM) and riverine (MQ) sites seem characterized by very  
 387 high carbohydrate peaks ( $1030\text{ cm}^{-1}$ ), but a closer look at the wavenumbers reveal a probable influence by silicate compounds  
 388 ( $1005$  and  $912\text{ cm}^{-1}$ ), which is confirmed by the presence of kaolinite peaks ( $3620$  and  $3695\text{ cm}^{-1}$ ). Given that the mangrove and  
 389 riverine sites are prone to flooding, it is perhaps not surprising to see this overprint by mineral compounds, but those peaks obscure  
 390 the carbohydrate signature (Verbeke et al., 2022). The mangrove site also presented low aromatic ( $1510$  and  $1630\text{ cm}^{-1}$ ) and  
 391 aliphatic peaks, which can be interpreted as indicating a lower degree of humification when compared to the coastal swamp and  
 392 the montane peatbog.  
 393



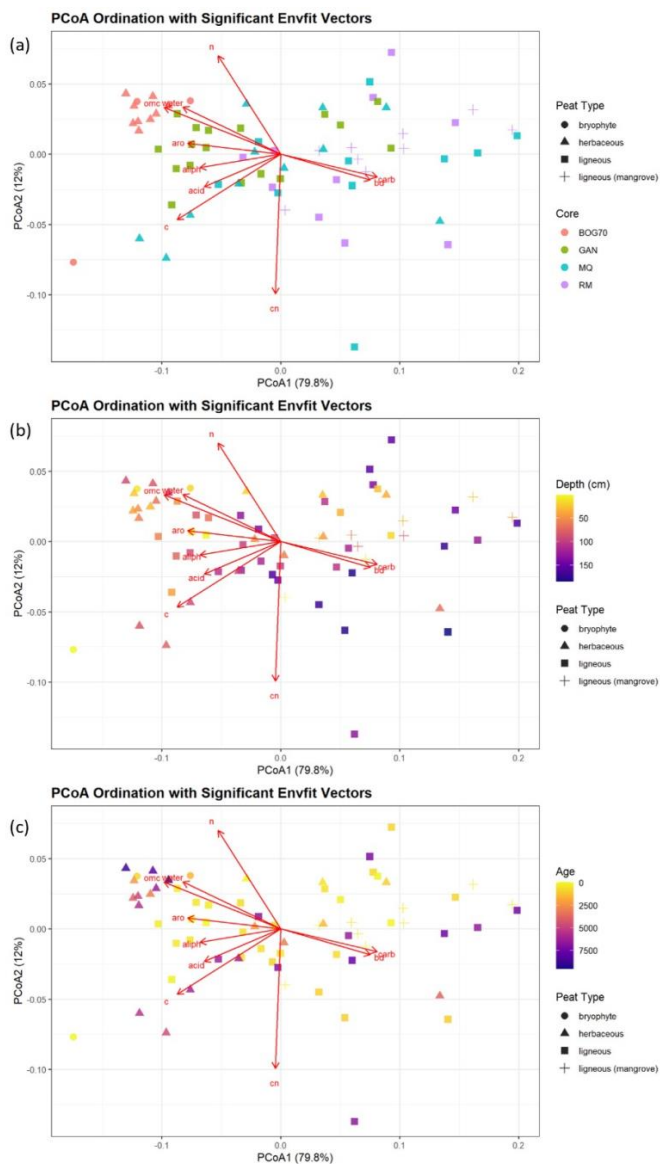
394

395 **Figure 7. Average FTIR spectrum from our four full cores from Costa Rica.**

396 **3.2.2 Differences in peat composition and properties across sites**

397 Peat composition and properties differ among the four sites (Fig. 8 and A7; Table A2), likely due to differences in organic matter  
398 quality. The first PCoA axis, explaining 79.8% of the observed variation, places %C as well as the aromatics, aliphatics, and acids  
399 on the left side of the ordination vs. the carbohydrates and BD on the right side of the ordination, as expected. The second axis  
400 (12%) was not strongly linked to any environmental variables. The PCoA plot showed that the peat properties from most samples  
401 from the montane peatbog (BOG70) and the coastal peat swamp (GAN) sites can be distinguished from those of the other two  
402 sites. In contrast, the mangrove (RM) and riverine (MQ) sites, regardless of peat type, depth, or age (Fig. A7), were scattered across  
403 the horizontal axis. Lastly, the PCoA plot that has the samples color-coded by depth (Fig. A7) shows a cluster of the shallower  
404 samples towards the left-hand side of the statistical space, suggesting the role of age on peat properties.

405



406

407

408

**Figure 8. Principal Coordinates Analysis (PCoA) using Bray-Curtis distances overlaid with envfit vectors. The data in the ordination are visualized by (a) peat type and core, (b) peat type and depth, and (c) peat type and age.**

409

We note that bulk density and carbohydrates seem to covary (Fig. 8, on the right-hand side of axis 1). The expectation is that carbohydrate relative abundance would be negatively correlated with bulk density, but the ordination instead suggests a strong positive relationship between those two variables. We posit that this unexpected result may reflect the contribution of Si-O bands from clay minerals in the C-O region at  $\sim 1030\text{ cm}^{-1}$ , confounding carbohydrates with silicates in the spectra (Fig. 7; Fig. A3 and A4). With mineral contributions enhancing the signals of both carbohydrate relative abundance and bulk density, those parameters may co-vary in mineral-rich samples.

414



415

416 Subsequent PERMANOVA analysis (Table A3) revealed differences between sites ( $R^2 = 0.434$ ,  $F_{3,65} = 16.64$ ,  $p \leq 0.001$ ) and  
417 among peat types ( $R^2 = 0.282$ ,  $F_{3,65} = 8.52$ ,  $p \leq 0.001$ ), explaining 43.4 and 28.2% of the variation in the Bray-Curtis ordination,  
418 respectively. When tested together, site and peat type explained 50.1% of the variation ( $R^2 = 0.501$ ,  $F_{6,62} = 10.38$ ,  $p \leq 0.001$ ). The  
419 homogeneity of dispersion (betadisper), which shows the internal variation within each group, was determined for both sites ( $F_{3,65}$   
420  $= 5.21$ ,  $p = 0.003$ ) and peat types ( $F_{3,65} = 1.63$ ,  $p = 0.19$ , Fig. A8). Dispersion was shown to be significantly different across sites,  
421 with the mangrove (RM) and the riverine (MQ) sites displaying greater heterogeneity, but not significantly different among peat  
422 types.

423

424 Lastly, a distance-based redundancy analysis (dbRDA) constrained by site and peat type was run to constrain the community  
425 variables (Table A3). Site and peat type together ( $F_{6,62} = 8.253$ ,  $p \leq 0.001$ ) explained 44.4% of total dispersion in the Bray-Curtis  
426 ordination. The majority of the variation was explained by the sites themselves ( $F_{3,62} = 14.02$ ,  $p \leq 0.001$ ), with 'peat types' adding  
427 explained variance ( $F_{3,62} = 2.49$ ,  $p = 0.024$ ). A final pairwise PERMANOVA was run to determine which sites (Table A4) and peat  
428 types (Table A5) differed specifically from one another. Among the sites, all pairwise comparisons were statistically different from  
429 one another, except for MQ and RM ( $R^2 = 0.071$ ,  $F_{1,38} = 2.912$ ,  $p = 0.066$ ). The strongest difference was observed between BOG70  
430 and RM ( $R^2 = 0.667$ ,  $F_{1,29} = 58.764$ ,  $p = 0.0015$ ). Among peat types, all comparisons were statistically different, except for  
431 bryophyte and herbaceous peats ( $R^2 = 0.103$ ,  $F_{1,21} = 2.402$ ,  $p = 0.092$ ). Ligneous and ligneous (mangrove) showed strong  
432 differentiation from bryophyte (Ligneous:  $R^2 = 0.153$ ,  $F_{1,38} = 6.908$ ,  $p = 0.004$ ; Ligneous (mangrove):  $R^2 = 0.687$ ,  $F_{1,10} = 21.976$ ,  
433  $p = 0.009$ ) and herbaceous peats (Ligneous:  $R^2 = 0.144$ ,  $F_{1,55} = 9.275$ ,  $p = 0.004$ ; Ligneous (mangrove):  $R^2 = 0.412$ ,  $F_{1,27} = 18.924$ ,  
434  $p = 0.004$ ). Ligneous and ligneous (mangrove) did display significant differences from one another ( $R^2 = 0.090$ ,  $F_{1,44} = 4.343$ ,  $p =$   
435  $0.025$ ), but albeit at a lesser significance than bryophyte and herbaceous.

## 436 4 Discussion

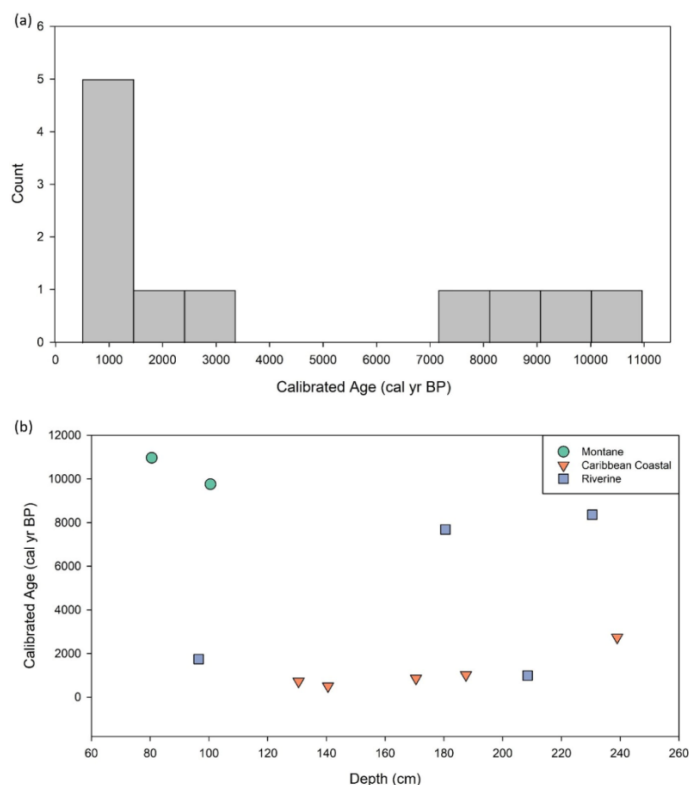
### 437 4.1 Peat inception ages and age-depth relationships of Costa Rican peatlands

438 The timing of peatland inception has been used in many studies worldwide to help constrain changes in hydroclimatic conditions  
439 (Dommain et al., 2014; Thomas et al., 2025; Yu et al., 2016). In the case of Costa Rica, the dataset shows a wide range of peat  
440 inception age, with no particular time period during which peats primarily initiated. Peat inception ages range from 507 to 10,967  
441 cal. yr BP (Fig. 9) and tend to cluster on the basis of peatland type / geomorphological setting. The montane peatlands exhibited  
442 the oldest ages, with BOG68 dating back to  $10,967 \pm 248$  cal. yr BP. Conversely, the youngest peatlands were observed along the  
443 Caribbean coast, with the coastal palm swamp near Limon (AIR site) only dating back to  $507 \pm 24$  cal. yr BP. The inland riverine  
444 sites encompass a wider age range, between  $988 \pm 64$  and  $8361 \pm 96$  cal. yr BP. A histogram combining all peat basal ages from  
445 this study suggests that most peatlands in Costa Rica are very young (less than 2000 years old), but this finding is partly due to a  
446 sampling artefact, as most of the sites are located in the coastal area. We have not found peats of pre-Holocene age in Costa Rica,  
447 a common theme across Latin America and the Caribbean (e.g., Lawson et al., 2026). Overall, the spatiotemporal pattern of peat  
448 inception primarily relates to elevation (high-elevation sites are the oldest) and proximity to the coast (coastal sites are the  
449 youngest).

450



451 While the age of the montane peatlands was likely constrained by deglacial processes (Horn, 1990), the relatively recent inception  
452 and expansion of peatlands along the Caribbean coast (~1000 cal. yr BP) was probably linked to increased stability in base level,  
453 which combines stable sea level conditions as well as lowered variability in freshwater and sediment inputs from the inland rivers  
454 that feed the coastal lowlands. Regional sea-level stabilization is thought to have taken place around 6000 cal. yrs BP (Castañeda-  
455 Posadas et al., 2022), suggesting that other local factors might have prevented peatland establishment or development along the  
456 coast for many thousands of years, such as dynamic floodplains, earthquakes, erosion caused by storms, etc. As for the riverine  
457 sites, our limited sampling does not allow us to generalize, but it seems that our three sites (MQ, SJ, LM) lay within a lowland area  
458 that used to be flooded by Lago Nicaragua (also known as Lago Cocibolca) (Fig. 3; Bergoeing and Protti, 2006). Holocene  
459 fluctuations in the lake level, which could have been caused by a changing climate as well as tectonic activity (Kutterolf et al.,  
460 2023; Slate et al., 2013), have likely caused large shifts in the hydrological regime of the studied wetland complexes that span  
461 hundreds of km<sup>2</sup> in the area. Alas, the general lack of paleodata from the region makes it difficult to further address the cause and  
462 timing for peatland inception, though a 5700-year-old record from Lago Nicaragua reveals a potential impact of pre-colombian  
463 agriculture (5400 cal. yr BP) on the region as well as a general drying trend throughout the mid- to late-Holocene (Slate et al.,  
464 2013).  
465



466

467

468

**Figure 9. Peat inception ages from Costa Rican peatlands. (a) Peat initiation frequency distribution, presented in 1000-yr bins, (b) peat basal age vs. depth. The ecosystem types are displayed using different symbols and colors.**



469

470 Two of our study sites combine a full core and a bottom core, allowing us to provide some preliminary information on the spatio-  
471 temporal pattern of peatland expansion in Costa Rican peat basins. In the coastal site Gandoca (GAN), two cores were retrieved  
472 towards opposite ends of a 1 km long transect that runs perpendicular to the ocean. The full core (GAN) is located close to the  
473 beach and is characterized by 130 cm of peat that is aged at 668 cal. yr BP. Near the other end of the transect is core GAN-SF,  
474 with 170 cm of peat that dates back to 863 cal. yr BP. Those results point to a somewhat homogeneous back-barrier depression  
475 that could have filled up more or less synchronously. This preliminary finding is supported by our probe peat depth data points  
476 along the GAN transect ( $n = 10$ ), which are all between 130 and 170 cm. Interestingly, we found a similar depth pattern at the AIR  
477 site, with peat depth values around 140 cm ( $n = 7$ ).

478

479 In riverine wetland complex Medio Queso (MQ), 2 cores were also collected along a 600 m long, west-east transect from the edge  
480 of the site towards Rio Medio Queso. The full core (MQ; depth = 180 cm, age = 7683 cal. yr BP) and the bottom core (MQ-10;  
481 depth = 230 cm; age = 8361 cal. yr BP) are located approximately 100 m apart, with MQ-10 closer to the river. At this site, deeper  
482 (and likely older) peats are found along the transect, as corroborated by the probing depths ( $n = 10$ ), which start at 40 cm near the  
483 edge of the site and reach 230 cm near the river, suggesting a progressive infilling of a local depression bordering the river.

484

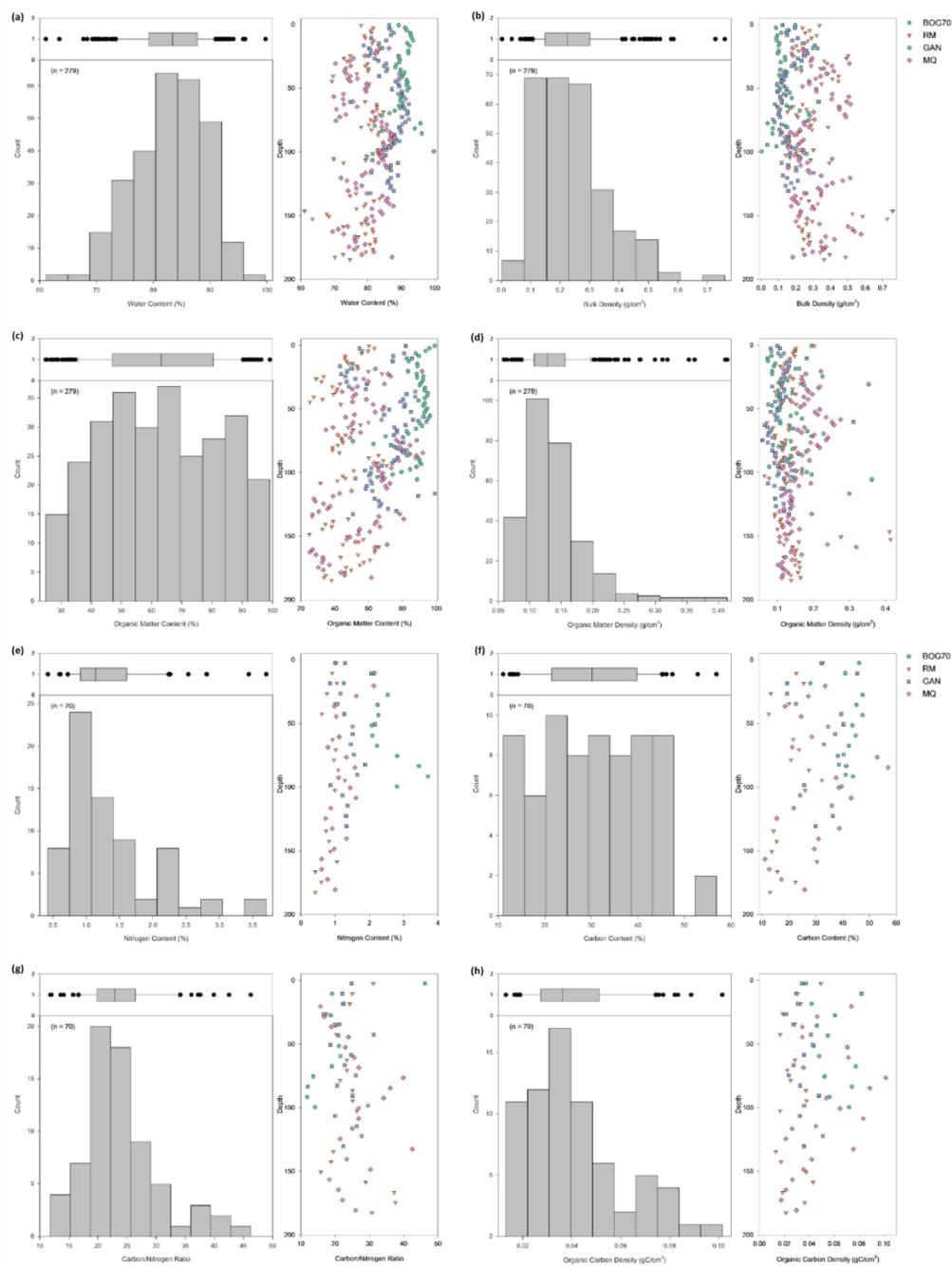
485 Long-term apparent rates of peat accumulation also vary across peatland types and geomorphological settings (see age-depth  
486 models on Fig. 2-5). The nearly 10,000-year-old, but shallower (100 cm deep) montane site (BOG70) was characterized by an  
487 average apparent rate of peat accumulation (0.01 cm/yr) that is an order of magnitude slower than its coastal lowland counterparts.  
488 Indeed, the coastal peat swamp site (GAN) accumulated 130 cm of peat in only about 700 years; similarly, the mangrove site (RM)  
489 accreted 185 cm of peat in about 1000 years. The nature of the peat deposits differs across these sites: herbaceous at BOG70 vs.  
490 ligneous at GAN and RM, which might factor in the variations reported above. The differences in climatic regimes between the  
491 cool, high-altitude montane sites vs. the warm, lowland sites could also explain the reported differences in peat accumulation rates,  
492 with the cooler conditions acting as a limit to plant productivity. A third, and non-exclusive, process at play is that of long-term  
493 peat accumulation itself: the oldest peat (montane site) has had much more time to decompose, albeit slowly, than the material  
494 found in at the younger sites. With all that said and despite these large differences in accumulation rate, the organic carbon density  
495 was similar across all sites (mean = 0.04 gC/cm<sup>3</sup>). The stratigraphies were also all characterized by large amounts of recalcitrant  
496 compounds (aromatics and aliphatics), suggesting that the peat carbon store is stable and thus somewhat protected from further  
497 mineralization, regardless of age and peat type.

#### 498 **4.2 Geochemical characterization of Costa Rican peatlands**

499 Combining all the loss-on-ignition measurements ( $n = 279$ ) and elemental analysis data ( $n = 70$ ) across our four cores provides an  
500 overview of peat water content, dry bulk density, organic matter content, organic matter density, carbon and nitrogen content, and  
501 C/N ratio for Costa Rican peatlands. Table 3 and Fig. 10 present the data ranges as well as the mean values and standard deviation  
502 for all those variables. One-way analyses of variance (ANOVA) revealed that all peat types were statistically different from each  
503 other in the case of water content ( $F_{2,276} = 11.94$ ,  $p < 0.0001$ ) and organic matter content ( $F_{2,276} = 44.66$ ,  $p < 0.0001$ ). In the case of  
504 dry bulk density, the ANOVA revealed an overall effect of peat type ( $F_{2,276} = 4.95$ ,  $p < 0.01$ ), with the bryophyte type significantly  
505 different (Tukey's LSD:  $p < 0.001$ ) from herbaceous and ligneous peats. Lastly, for organic matter density, we also report an



506 overall effect of peat type ( $F_{2,276} = 18.38$ ,  $p < 0.0001$ ), with the herbaceous peat type significantly different (Tukey's LSD:  $p <$   
507  $0.001$ ) from the bryophyte and ligneous peat types. Statistical tests were not applied to %C, %N, and C/N, given the lower number  
508 of samples available. We also note that the correlation between %C and %OM in the Costa Rican samples was strong and  
509 statistically significant (Spearman correlation = 0.847;  $p < 0.0001$ , Fig. 11). The slope (0.51) of the linear regression indicates that  
510 %C is about half the OM content, similar as the relationship found in the northern peatland database for non-*Sphagnum* peat (0.514;  
511 Loisel et al. 2014), supporting the idea that OM content and %C are closely related in peatlands across biomes, despite the large  
512 differences in their relative geochemical characteristics.



513

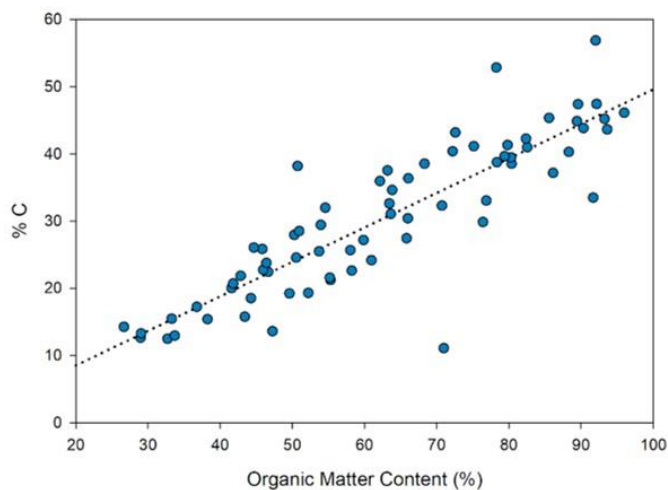
514

515

516

**Figure 10:** Frequency distribution histograms and downcore profiles of peat properties in Costa Rican peatlands. (a) Water content (%), (b) bulk density ( $\text{g}/\text{cm}^3$ ), (c) organic matter content (%), (d) organic matter density ( $\text{g}/\text{cm}^3$ ), (e) nitrogen content (%), (f) carbon content (%), (g) carbon/nitrogen ratio, and (h) organic carbon density ( $\text{gC}/\text{cm}^3$ ).

517



518

519

**Figure 11: Relationship between organic matter content and carbon content in Costa Rican peat.**

	Mean	Variance ( $\sigma^2$ )	Minimum	Maximum
Water Content (%)	82.90	41.74	61.07	99.77
Bulk Density ( $\text{g}/\text{cm}^3$ )	0.242	0.015	0.003	0.759
Organic Matter Content (%)	63.10	383.05	24.99	99.14
Organic Matter Density ( $\text{g}/\text{cm}^3$ )	0.139	0.003	0.059	0.414
Nitrogen Content (%)	1.358	0.448	0.421	3.705
Carbon Content (%)	30.463	125.145	11.065	56.870
Carbon/Nitrogen Ratio	23.983	44.968	11.830	46.466
Organic Carbon Density ( $\text{gC}/\text{cm}^3$ )	0.0418	0.0004	0.0131	0.1014

520

**Table 3: Descriptive statistics for Costa Rican peat geochemical properties.**

521

Combining the geochemical data together by peat type (bryophyte, ligneous, herbaceous) provides the first dataset of its kind for

522

Costa Rica (and the Caribbean more broadly), with direct usability for regional carbon analysis and modeling (Fig. 12). Bryophyte

523

peat ( $n = 10$ , only coming from the montane site) is characterized by high organic matter content ( $86 \pm 14\%$ ), the highest of all

524

peat types. This result is approximately 10% lower than, though still in line with, results from the northern hemisphere peatland

525

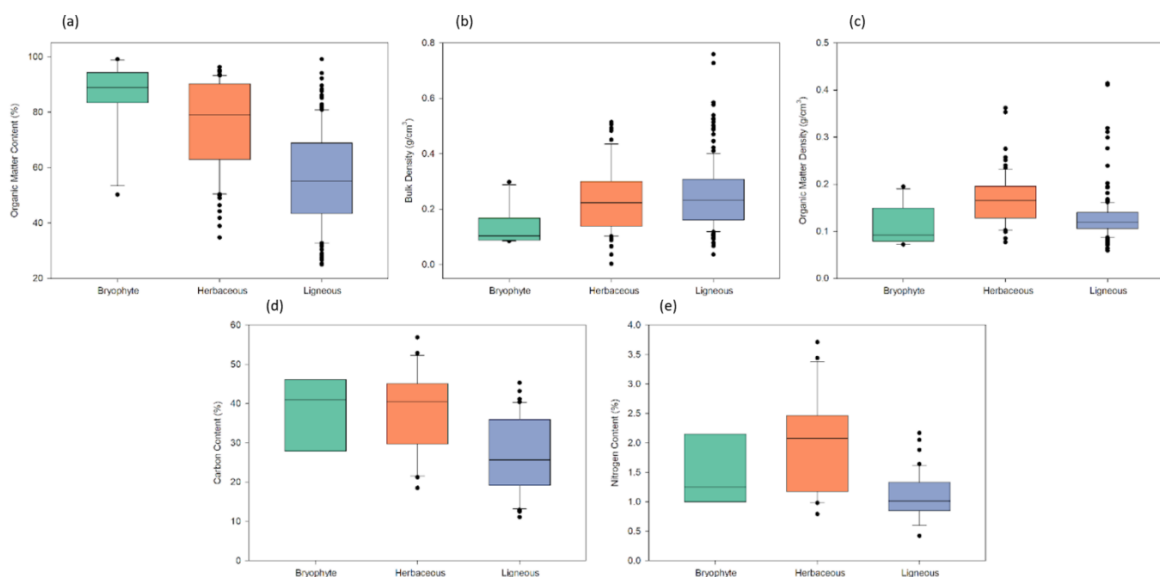
database ( $94 \pm 9\%$ ; Loisel et al. 2014). As for bulk density and organic matter density, the Costa Rican bryophyte peats are about

526

60% more dense than their northern counterparts (BD:  $0.13 \pm 0.07$  and OMD  $0.11 \pm 0.04 \text{ g}/\text{cm}^3$  in Costa Rica vs.  $0.08 \pm 0.04$  and



527  $0.07 \pm 0.03 \text{ g/cm}^3$ ). Carbon and nitrogen content also differed between these populations: %C was lower ( $38 \pm 9\%$ ) than in the  
 528 northern peats ( $46 \pm 4\%$ ) whereas %N was about twice as high ( $1.5 \pm 0.6\%$  vs.  $0.7 \pm 0.3\%$ ). Herbaceous peat ( $n = 84$ , with data  
 529 coming from our montane and riverine sites) yielded moderately high organic matter content ( $75 \pm 17\%$ ). Compared to northern  
 530 herbaceous peats, Costa Rica is approximately 10% lower ( $86 \pm 15\%$ ). Costa Rican peats are about 50% more dense than their  
 531 northern counterparts, in terms of both bulk density and organic matter density (BD:  $0.23 \pm 12$  and OMD:  $0.15 \pm 0.05 \text{ g/cm}^3$  in  
 532 Costa Rica vs.  $0.12 \pm 0.08$  and  $0.09 \pm 0.04$ ). %C in herbaceous Costa Rican peats were lower ( $38.5 \pm 10.3\%$ ) than in northern  
 533 peats ( $50.5 \pm 4.9\%$ ); %N was only slightly higher in Costa Rica ( $2 \pm 0.8\%$ ) than in the north ( $1.7 \pm 0.6$ ). Ligneous peat ( $n = 185$ ,  
 534 with data from the riverine, coastal swamp, and mangrove) yielded around 30% lower organic matter content ( $56 \pm 17\%$ ) than  
 535 northern ligneous peats ( $92 \pm 14\%$ ). Bulk density and organic matter density from ligneous peats was higher in Costa Rica than in  
 536 the north (BD:  $0.25 \pm 12$  and OMD:  $0.13 \pm 0.05 \text{ g/cm}^3$  in Costa Rica vs.  $0.11 \pm 0.05$  and  $0.1 \pm 0.03$ ). %C was almost double in  
 537 northern peatlands ( $50.9 \pm 4.0\%$ ) than in Costa Rica ( $26.7 \pm 9.8\%$ ). %N was also higher in ligneous northern peats ( $1.3 \pm 0.5\%$ )  
 538 than in Costa Rica ( $1.1 \pm 0.4\%$ ).  
 539



540  
 541 **Figure 12: Box plots of geochemical data by peat type. (a) Organic matter content (%), (b) bulk density ( $\text{g/cm}^3$ ), (c) organic matter**  
 542 **density ( $\text{g/cm}^3$ ), (d) carbon content (%), and (e) nitrogen content (%).**

### 543 4.3 Costa Rican peatland carbon stock

544 To estimate peat carbon storage, previous studies have often reverted to a simple formula that combines peat extent, average peat  
 545 depth, average bulk density, and an assumed carbon content of 50 or 51% (Gorham, 1991; Loisel and Yu, 2013; Yu et al., 2010).  
 546 Here, we used a peatland extent of  $1,456 \text{ km}^2$  (Rabel et al., 2025), an average peat depth of 150 cm (which is the average depth for  
 547 the 9 sites presented in this study), an average bulk density of  $0.24 \text{ gC/cm}^3$  and an average carbon content of 30%. These values  
 548 yielded a peat carbon store of  $1.573 \times 10^{14} \text{ g C}$ , or 0.1573 Gt C.  
 549



550 Of course, every one of the values used above carries uncertainties, starting with the peatland extent, which was performed using  
551 a probabilistic approach (Rabel et al. 2025) that may under- or over-estimate the extent. Illustrating this uncertainty is the range of  
552 peat extent for Costa Rica that was provided in previous (global) peat mapping efforts, from 577 to 2670 km<sup>2</sup> (Melton et al., 2022;  
553 UNEP, 2022). Using these peatland extents results in carbon stores ranging between 0.0623 and 0.2883 Gt C for Costa Rican  
554 peatlands. An important aspect to highlight is that previous peat-carbon store estimates often use 0.1 g/cm<sup>3</sup> as their bulk density in  
555 combination with an assumed 50% carbon content, yielding an organic carbon density of 0.05 gC/cm<sup>3</sup>. The results for Costa Rica  
556 suggest an organic carbon density of 0.072 gC/cm<sup>3</sup> (0.24 g/cm<sup>3</sup> \* 30%), about 30% greater than the previous value. While this  
557 result should be further confirmed through additional measurements, it cautions against the broad application of well-established  
558 knowledge from extra-tropical peatlands to discuss peat-carbon characteristics in tropical peatlands. Estimates created out of those  
559 values would greatly underestimate the tropical carbon store.

#### 560 4.4 Peatland successional pathways in Costa Rica

561 Ecological succession can be inferred from the plant macrofossil results. It is noteworthy that three out of our four study sites  
562 started as palm swamps (GAN, RM, MQ). While GAN has remained a palm swamp throughout its development (800 years), the  
563 mangrove site (RM) switched from palm to mangrove around 540 years ago. While ecological succession in wetlands and peatlands  
564 tends to go from wetter to drier environments, there exist many examples of opposite trends (from drier to wetter) that can be  
565 caused by changes in local hydrology that might have been induced by a lowering of the base level (land subsidence, sometimes  
566 caused by earthquakes or large erosional storms such as hurricanes) or an increase in sea level (causing flooding and saltwater  
567 intrusion) (McCloskey and Liu, 2012; Phillips and Bustin, 1996; Urquhart, 2009; Urrego et al., 2019). The coastal area where our  
568 mangrove site is located is both geomorphologically and tectonically active, with an estuary in close proximity and a history of  
569 paleo-earthquakes (Denyer, 1998). As for the riverine site (MQ), the switch from palm swamp to herbaceous peatland took place  
570 around 5500 years ago and suggests a transition into a drier (though still wet) environment. The river that transects this peatland  
571 complex (Rio Medio Queso) is a tributary of Rio San Juan, itself a major outlet of Lago Nicaragua (Fig. 3). Mid-Holocene  
572 fluctuations in the lake level would have likely caused large shifts in the hydrological regime and botanical nature of the regional  
573 wetland complexes that span hundreds of km<sup>2</sup> in the area. Unfortunately, there is a lack of paleodata from the lake to corroborate  
574 with the peat core.

575  
576 The montane peatland presented a different story. The BOG70 core indicates a recent switch from herbaceous to bryophyte peat  
577 that might have taken place within the past few decades (Fig. 5a). It is important to note that the modern ecological assemblage of  
578 the peatland is unusual for Costa Rica; *Sphagnum* and lichen species are typically found in cool environments of the mid- and  
579 high-latitude regions of the world. Atop the Cordillera de Talamanca, where the site is found, temperatures are cool and much of  
580 the moisture is brought in the form of fog (cloud forest). The little evidence of Holocene-scale changes in paleoclimate in this area  
581 comes from a lake study (Lago Morrenas) that shows a mesic early Holocene, followed by wetter conditions during the middle  
582 Holocene, and high variability throughout the late Holocene (Kerr et al., 2024). It is possible that regional changes in hydroclimate  
583 have allowed for *Sphagnum* peat to develop here. However, the lake-based palynological record available for the region does not  
584 indicate clear shifts in vegetation in the late Holocene (Horn, 1993).

#### 585 4.5 Peat type as a driver of organic matter quality in Costa Rica



586 It has been shown that tropical lowland peats typically contain high levels of aromatics and low levels of carbohydrate compounds,  
587 indicative of humified, but stable, conditions that allow for long-term carbon accumulation and storage (Hodgkins et al., 2018;  
588 Verbeke et al., 2022). Our results generally corroborate the finding that tropical peat deposits contain substantial relative abundance  
589 of aromatic (and aliphatic) components.

590

591 The effect of peat type on the nature of the peat carbon compounds is worth discussing. But first, we note that peat was generally  
592 very humified throughout all the profiles (von Post and C/N), except for the near surface of BOG70 and one thin layer in RM,  
593 making correlations with our FTIR data challenging. As for peat types, our analysis indicates a much greater abundance of aliphatic  
594 compounds in the herbaceous peat when compared to the other types, suggesting a potential signature for herbaceous plants. The  
595 relationships between OM content, aliphatics, and aromatics were firmly positive, confirming that stable components are  
596 controlling organic matter accumulation (e.g., Hodgkins et al., 2018; Leri et al., 2025; Verbeke et al., 2022).

597

598 The anticipated effect of depth (and age) on the carbon compounds was not straightforward. The relative abundance of  
599 carbohydrates was expected to decrease downcore (representing a progressive decay of those labile compounds) and in turn induce  
600 relative increases in the more stable components of organic matter (aromatics and aliphatics) (Broder et al., 2012; Tfairly et al.,  
601 2014; Upton et al., 2018). We identified those trends at the montane (BOG70) and the coastal peat swamp (GAN) sites. However,  
602 in the case of the riverine (MQ) and mangrove (RM) sites, no such trends along-core were discerned. While it is possible that the  
603 nature of some tropical peats does not lend itself to those trends, as the organic matter mineralizes very quickly (i.e., near the top  
604 of the soil profile), the interference of silica in the carbohydrate signature could have also further hindered the visibility of those  
605 expected relationships with depth by creating anomalously high carbohydrate peaks where, in reality, little carbohydrates were to  
606 be found.

607

608 Lastly, it is worth mentioning the potential importance of root biomass in the process of carbon accumulation at our study sites.  
609 While we did not quantify root contribution to the peat mass (those analyses will be underway shortly), it is clear from the plant  
610 macrofossil analysis that the peat itself is often almost entirely composed of fine roots, as observed in other tropical settings  
611 (Chimner and Ewel, 2005). These fine roots have been previously shown to be the driving contributor of organic matter  
612 accumulation in some mangrove systems (Liu et al., 2017; McKee et al., 2007; Middleton and McKee, 2001; Xiong et al., 2017)  
613 and tropical riverine swamps (Sciumbata et al., 2023). A high ratio of root contribution to the peat mass would support the  
614 hypothesis that tropical peatlands primarily rely on belowground organic matter inputs, in contrast with the more classic acrotelm  
615 / surface litter contribution to a growing mound where the water table rises and engulfs the dead plant matter (Clymo, 1984).

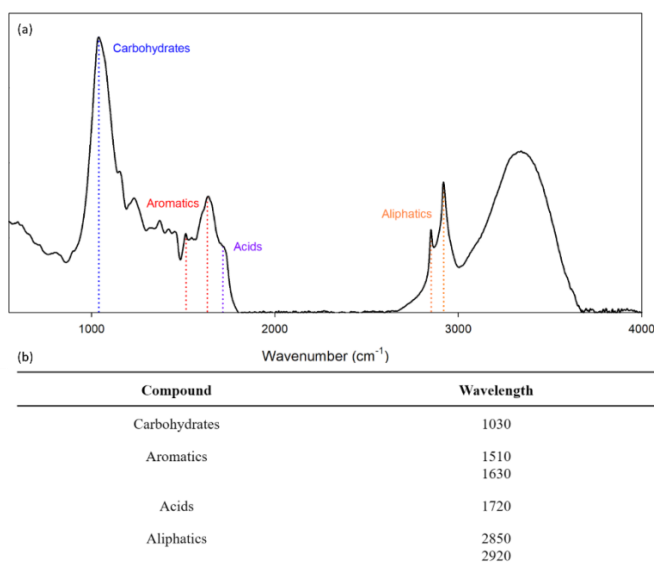
## 616 **5 Conclusions and future work**

617 This study offers the first systematic analysis of peat sediments for Costa Rica. The lab-based work presents important new datasets  
618 on peat geochemical properties (bulk density, organic matter content, carbon and nitrogen content). A key finding is that bulk  
619 density values tend to be greater in tropical lowland peatlands than what is typically reported for extra-tropical peatlands. The  
620 infrared spectroscopy confirms the mineralized, stable nature of the tropical peats, both in the lowlands and at high-elevation sites.  
621 Importantly, this observation applies across our four (diverse) sites, regardless of peatland type, age, or geomorphological setting,  
622 suggesting that rapid and intensive mineralization within the uppermost portion of the peat profile may lead to long-term carbon



623 storage. Aliphatic compounds were found in much greater abundances in herbaceous-dominated peatlands than the other types,  
 624 suggesting that their presence could potentially be used as a signature for this herbaceous peat. In terms of peatland dynamics, a  
 625 broad range of peatland inception ages were found across Costa Rica. Spatiotemporal patterns are thus far related to peatland type,  
 626 with older peats found in the montane region, intermediate and variable peat ages found along inland, river floodplains, and young  
 627 peats found along the coast. Averaged apparent rates of peat accumulation in the lowlands have been rapid and steady over time,  
 628 with age-depth models generally displaying linear trends, likely due to the humified nature of peat. High-elevation peat has  
 629 accumulated at a markedly lower rate than the lowland sites, most likely because of the temperature limitation on plant production  
 630 as well as the older age of those peat deposits. Lastly, the total peat carbon store in Costa Rica is estimated at 0.1573 gigatonnes,  
 631 on the basis of our new analyses combined with a recent peatland probability map. Overall, this study provides critical, first of its  
 632 kind information on the characteristics of Costa Rican peats, deepening our overall knowledge on tropical peatlands.

633 **Appendix A**

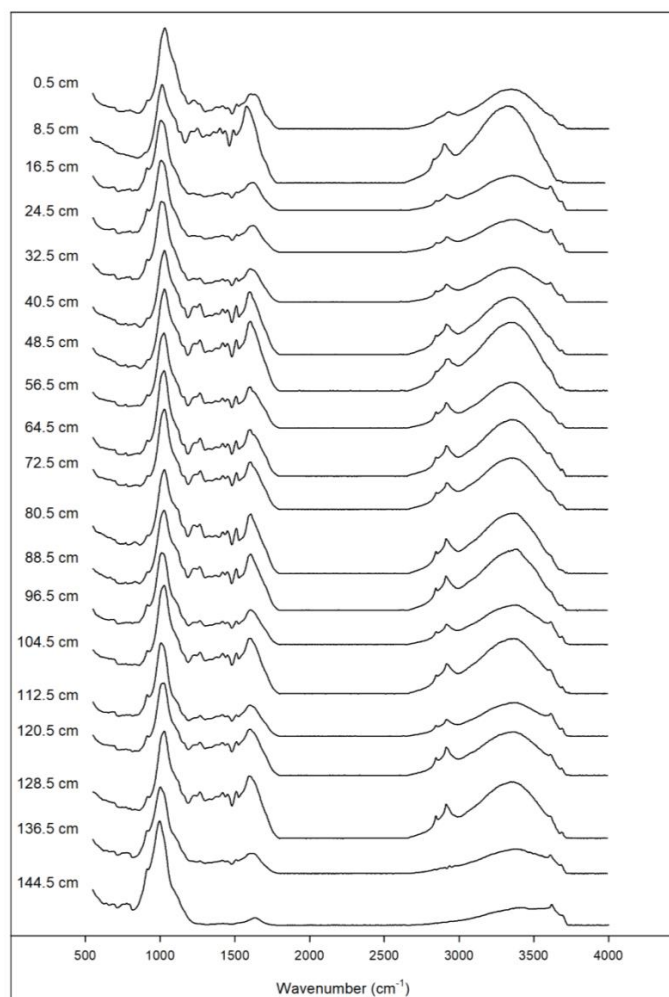


634

635 **Figure A1: Example of an FTIR spectra and peak finding for a peat sample. (a) The major functional compounds are identified after**  
 636 **baseline correcting and normalization within the custom R script, and (b) wavenumbers that relate to carbon compounds of interest.**



GAN Spectra



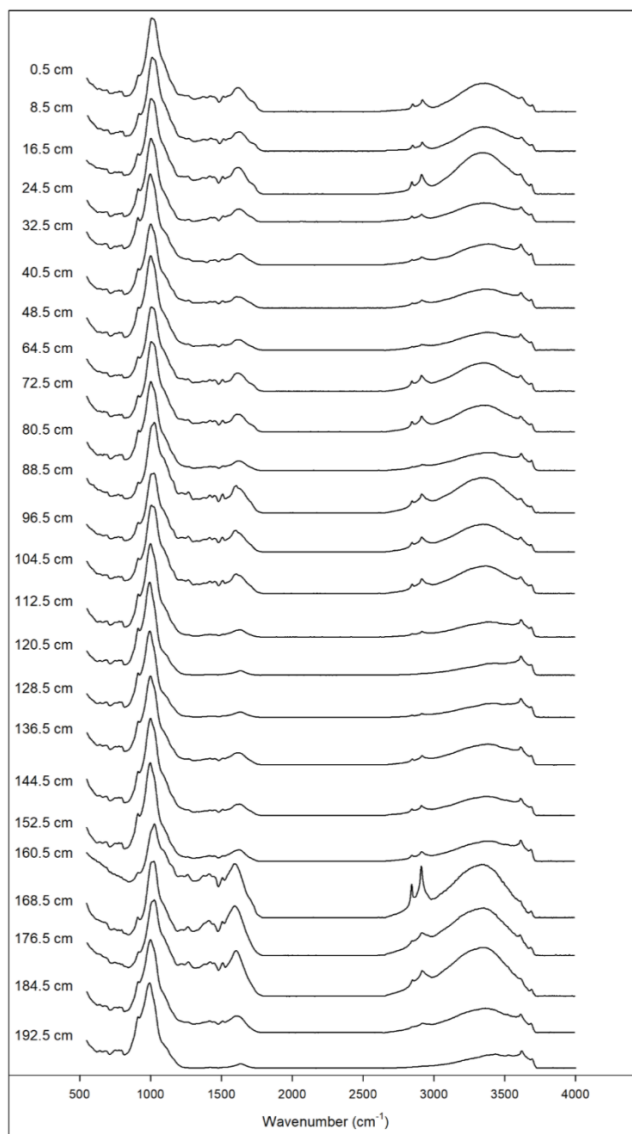
637

638

Figure A2: Stacked overlay of the FTIR spectra, GAN core.



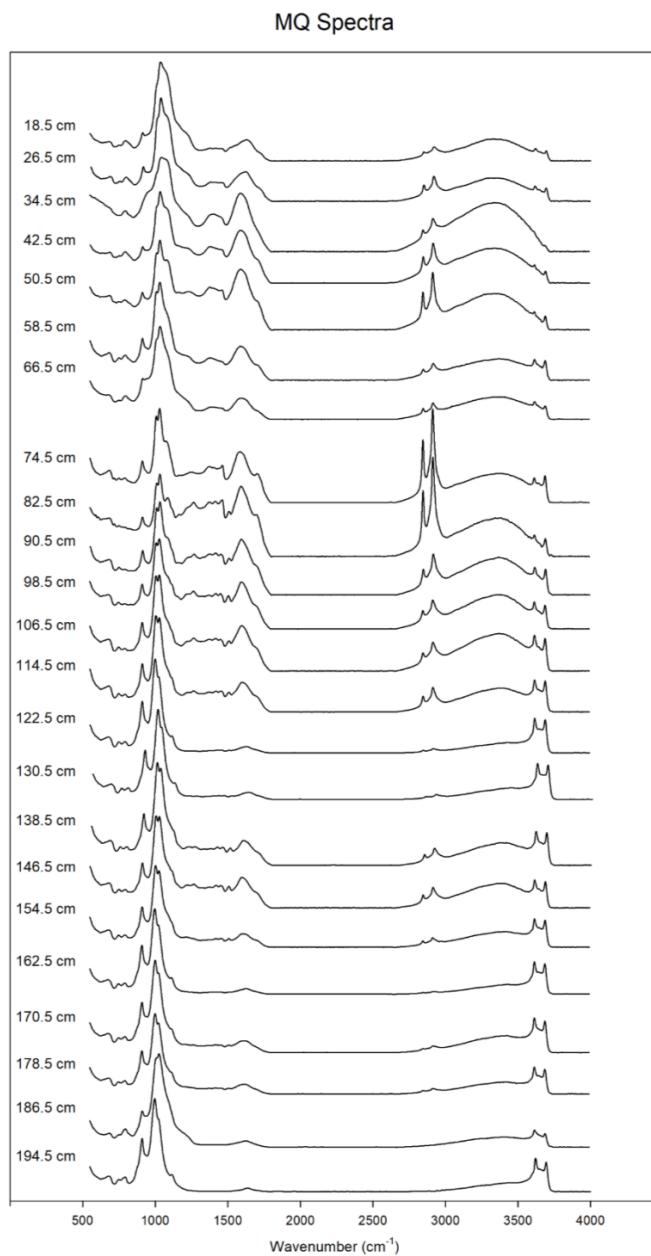
### RM Spectra



639

640

Figure A3: Stacked overlay of the FTIR spectra, RM core.

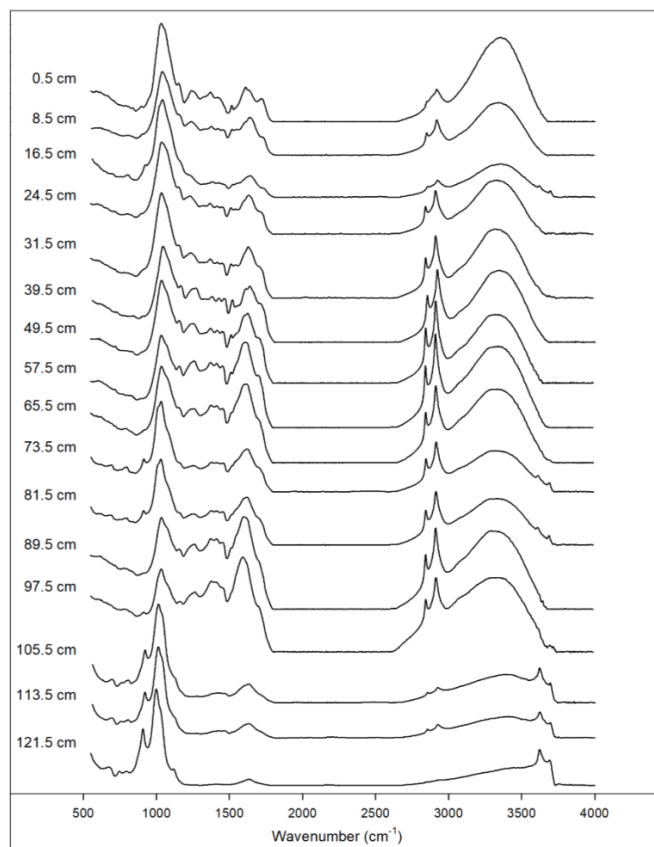


641

642 **Figure A4: Stacked overlay of the FTIR spectra, MQ core.**



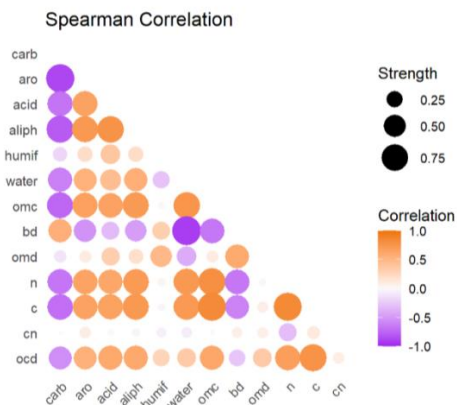
### BOG70 Spectra



643

644

Figure A5: Stacked overlay of the FTIR spectra, BOG70 core.



645

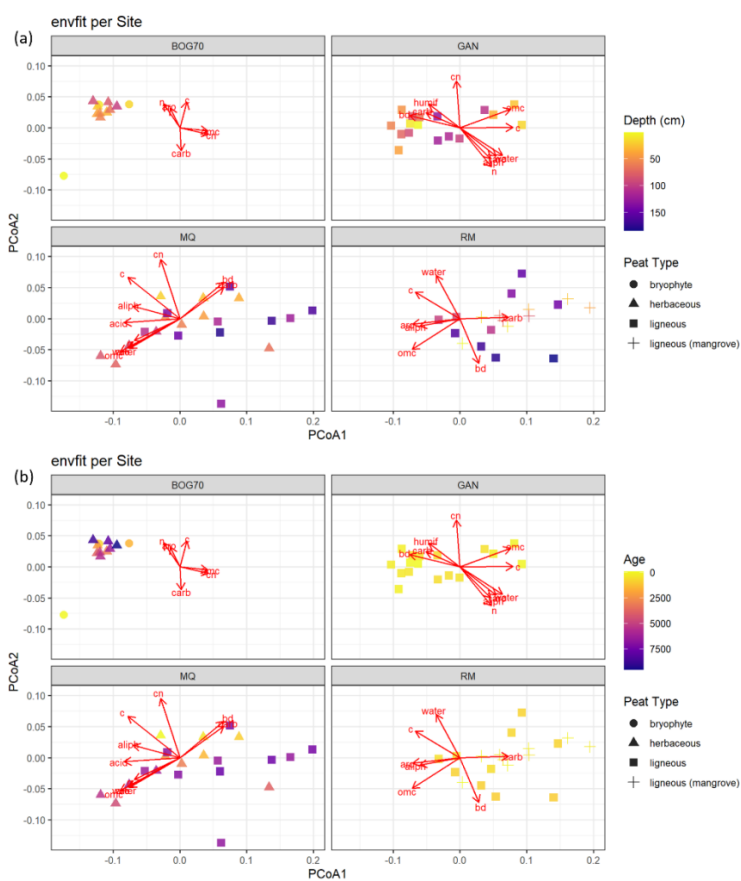
646

647

Figure A6: Spearman Correlation Matrix. Carb: carbohydrate; Aro: aromatic; Acid: acids; Aliph: aliphatics; Humif: humification; Water: water; Bd: bulk density; Omc: organic matter content; N: nitrogen; C: carbon; CN: Carbon/Nitrogen



648

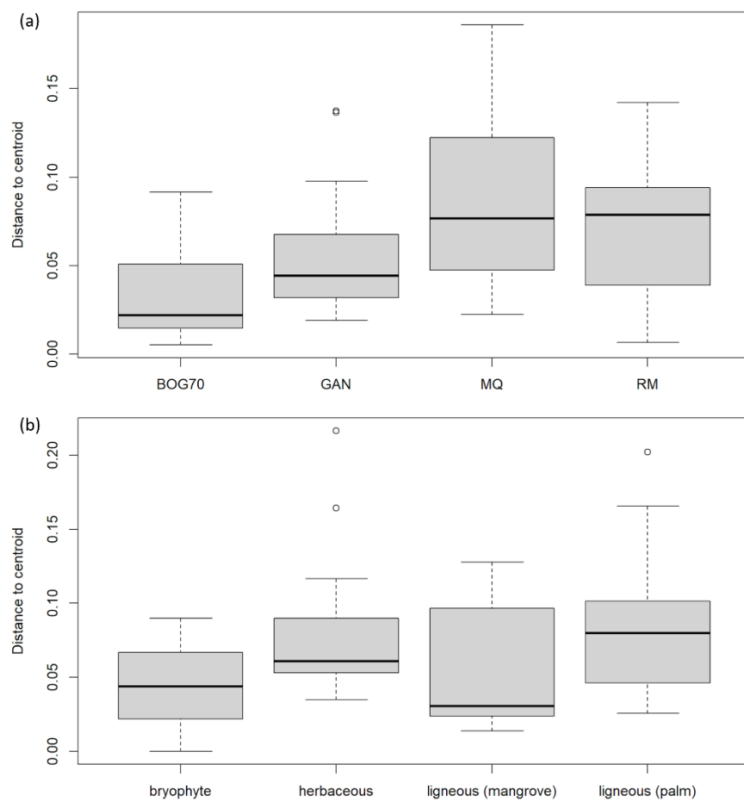


649

650

651

**Figure A7: Principal Coordinates Analysis (PCoA) using Bray-Curtis Distances overlaid by envfit vectors separated by core. The data in the ordination is additionally visualized by (a) depth and peat type and (b) age and peat type.**



652

653

Figure A8: (a) Betadisper box plot among cores, and (b) betadisper box plot among peat types

Proxy and Resolution	Cores
Loss-on-ignition (every 2 cm)	GAN-4 GAN-SF AIR MAN RM MQ-S9 MQ-S10 LM SJ BOG70 BOG68
Carbon & Nitrogen Content (every 8 cm)	GAN-4 RM MQ-S9 BOG70
von Post Humification Index (every 8 cm)	GAN-4 RM MQ-S9 BOG70
Macrofossil Composition (every 8 cm)	GAN-4



	RM MQ-S9 BOG70
Fourier-Transform Infrared Spectroscopy (every 8 cm)	GAN-4 RM MQ-S9 BOG70
Radiocarbon ( <sup>14</sup> C) Dating	GAN-4 GAN-SF AIR MAN RM MQ-S9 MQ-S10 LM SJ BOG70 BOG68

654 **Table A1: Summary of the proxies and analytical resolution used to analyze the Costa Rican peat cores.**

Variable	R <sup>2</sup>	p value	Significance
carb	0.607	≤ 0.001	***
aro	0.549	≤ 0.001	***
acid	0.415	≤ 0.001	***
aliph	0.417	≤ 0.001	***
humif	0.034	0.334	
water	0.704	≤ 0.001	***
bd	0.533	≤ 0.001	***
omc	0.952	≤ 0.001	***
n	0.682	≤ 0.001	***
c	0.866	≤ 0.001	***
cn	0.880	≤ 0.001	***

655 **Table A2: Statistical summary for the Environmental Fit (envfit) variables. Carb: carbohydrate; Aro: aromatic; Acid: acids; Aliph:**  
 656 **aliphatics; Humif: humification; Water: water; Bd: bulk density; Omc: organic matter content; N: nitrogen; C: carbon; CN:**  
 657 **Carbon/Nitrogen**

Test	Factor(s)	Df	Sum of Squares	R <sup>2</sup>	F	p-value	Significance
PERMANOVA	Core	3	0.31453	0.434	16.64	≤ 0.001	***



	Peat type	3	0.20441	0.282	8.52	≤ 0.001	***
	Core + Peat type	6	0.36289	0.501	10.38	≤ 0.001	***
<b>Betadisper (dispersion)</b>	Core	3	0.02396	–	5.21	0.003	**
	Peat type	3	0.00962	–	1.63	0.192	
<b>dbRDA</b>	Core + Peat type	6	0.378	0.444	8.25	≤ 0.001	***
	Core	3	0.321	–	14.02	≤ 0.001	***
	Peat type	3	0.057	–	2.49	0.024	*

658 **Table A3: Statistical summary for PERMANOVA, Betadisper, and dbRDA analyses. The significance levels are reported as follows: \* =**  
 659 **0.05, \*\* = 0.01, \*\*\* = 0.001**

Core 1	Core 2	R <sup>2</sup>	F	p-value	Significance
BOG70	GAN	0.365963	15.58425	0.0015	**
BOG70	MQ	0.444373	24.79284	0.0015	**
BOG70	RM	0.669569	58.76417	0.0015	**
GAN	MQ	0.129964	5.377604	0.0168	*
GAN	RM	0.331023	16.82385	0.0015	**
MQ	RM	0.071174	2.911872	0.066	

660 **Table A4: Statistical summary for pairwise PERMANOVA among cores.**

Peat type 1	Peat type 2	R <sup>2</sup>	F	p-value	Significance
bryophyte	herbaceous	0.102651	2.402275	0.092	
bryophyte	ligneous	0.15383	6.908256	0.004	**
bryophyte	ligneous (mangrove)	0.68727	21.97643	0.009	**



herbaceous	ligneous	0.1443	9.274842	0.004	**
herbaceous	ligneous (mangrove)	0.412068	18.92369	0.004	**
ligneous	ligneous (mangrove)	0.089831	4.342661	0.0252	*

---

661 **Table A5: Statistical summary for pairwise PERMANOVA among peat types.**

662 **Data availability**

663 The data will be made publicly available through Zenodo upon publication of this study.

664

665 **Author contributions**

666 JL conceptualized the study; HM, JL, and ACL performed the data analysis; HM and MA performed the labwork; JL, HM, MA,  
667 and JRW completed the fieldwork and acquired the samples; JL administered the project; HM and MA completed the study  
668 visualizations (figures); HM wrote the original draft; HM, JL, JRW, ACL, and MA contributed to manuscript editing and review.

669

670 **Disclaimer**

671 Copernicus Publications remains neutral with regard to jurisdictional claims made in the text, published maps, institutional  
672 affiliations, or any other geographical representation in this paper. While Copernicus Publications makes every effort to include  
673 appropriate place names, the final responsibility lies with the authors. Views expressed in the text are those of the authors and do  
674 not necessarily reflect the views of the publisher.

675

676 **Acknowledgements**

677 Thank you to Dr. Jan Peters, Dr. Cosima Tegetmeyer, Dr. Nick Girkin, Marko Stojanovic, Dr. Andrew Parsekian, Alexandra  
678 Peterson, Francisco Miranda, Haniel Rodriguez Roja and his family, and the SINAC officials in the conservation areas of La  
679 Amistad Caribe, Central, and Huetar Norte for professional help in our field expedition. Thank you to Emily Rabel, Dr. Nataleigh  
680 Perez, Lucy Barkis, Samantha Trexler, Kaitlan Gil-Najarro, April Reyes, and Patrick Campbell for their assistance in the field.  
681 Thanks also go to Easton Smith, Hope Serfoss, Josiah Marquez, Dr. Stephen Spain, Dr. Karis McFarlane, Dr. Adam Csank, Dr.  
682 Benjamin Sullivan, and Chloe Sileo for laboratory help, sample processing, and discussions about the content of this manuscript.  
683 Lastly, we acknowledge the Government of Costa Rica for site access and issuance of research (SE-DT-PI-026-2023), collection  
684 (SE-PI-LC-111-2023), and export permits (CUSBSE-157-2023) to JL.

685

686 **Financial Support**

<https://doi.org/10.5194/egusphere-2026-1209>

Preprint. Discussion started: 13 March 2026

© Author(s) 2026. CC BY 4.0 License.



687 This research was made possible by the National Science Foundation with awards #2142177 and #2406962 to JL. This work's

688 contents are solely of the authors and do not necessarily represent the official views of the National Science Foundation.

689

690 **Review Statement**



## References

- Álvarez-Sánchez, L. and Piedra-Castro, L. M.: Mangrove forests of the National Wildlife Refuge Gandoca-Manzanillo, Limón, Costa Rica, in: *Mangroves of Latin America*, UNIVERSIDAD ESPÍRITU SANTO, 2020.
- 695 Anderson, M. J.: A new method for non-parametric multivariate analysis of variance, *Austral Ecology*, 26, 32–46, <https://doi.org/10.1111/j.1442-9993.2001.01070.pp.x>, 2001.
- Artz, R. R. E., Chapman, S. J., Jean Robertson, A. H., Potts, J. M., Laggoun-Défarge, F., Gogo, S., Comont, L., Disnar, J.-R., and Francez, A.-J.: FTIR spectroscopy can be used as a screening tool for organic matter quality in regenerating cutover peatlands, *Soil Biology and Biochemistry*, 40, 515–527, <https://doi.org/10.1016/j.soilbio.2007.09.019>, 2008.
- 700 ASTM: *Standard Test Methods for Moisture, Ash, and Organic Matter of Peat and Other Organic Soils*, ASTM International, West Conshohocken, PA, 1987.
- Baird, A. J., Low, R., Young, D., Swindles, G. T., Lopez, O. R., and Page, S.: High permeability explains the vulnerability of the carbon store in drained tropical peatlands, *Geophysical Research Letters*, 44, 1333–1339, <https://doi.org/10.1002/2016GL072245>, 2017.
- Bergoing, J. P. and Protti, R.: Geomorfología Paleo-Lacustre del Sur del Lago de Nicaragua, *Revista Geográfica*, 27–38, 2006.
- 705 Biester, H., Knorr, K.-H., Schellekens, J., Basler, A., and Hermanns, Y.-M.: Comparison of different methods to determine the degree of peat decomposition in peat bogs, *Biogeosciences*, 11, 2691–2707, <https://doi.org/10.5194/bg-11-2691-2014>, 2014.
- Blaauw, M. and Christen, J. A.: Flexible paleoclimate age-depth models using an autoregressive gamma process, *Bayesian Analysis*, 6, 457–474, <https://doi.org/10.1214/11-BA618>, 2011.
- 710 Broder, T., Blodau, C., Biester, H., and Knorr, K. H.: Peat decomposition records in three pristine ombrotrophic bogs in southern Patagonia, *Biogeosciences*, 9, 1479–1491, <https://doi.org/10.5194/bg-9-1479-2012>, 2012.
- Camacho-Navarro, A., Herrera Zeledón, J. M., Vargas Alpizar, P., Jiménez Arce, R., Veas Ayala, N., Acuña Piedra, J. F., and Miranda Quirós, M.: Estado de los humedales: nuevos desafíos para su gestión. Contribución especial, Informe estado de la Nación en desarrollo humano sostenible, CONARE, 2017.
- 715 Castañeda-Posadas, C., Correa-Metrio, A., Escobar, J., Moreno, J. E., Curtis, J. H., Blaauw, M., and Jaramillo, C.: Mid to late Holocene sea-level rise and precipitation variability recorded in the fringe mangroves of the Caribbean coast of Panama, *Palaeogeography, Palaeoclimatology, Palaeoecology*, 592, 110918, <https://doi.org/10.1016/j.palaeo.2022.110918>, 2022.
- Chimner, R. A. and Ewel, K. C.: A Tropical Freshwater Wetland: II. Production, Decomposition, and Peat Formation, *Wetlands Ecol Manage*, 13, 671–684, <https://doi.org/10.1007/s11273-005-0965-9>, 2005.
- 720 Clymo, R. S.: The Limits to Peat Bog Growth, *Philosophical Transactions of the Royal Society of London. Series B, Biological Sciences*, 303, 605–654, 1984.
- Cobb, A. R., Dommain, R., Yeap, K., Hannan, C., Dadap, N. C., Bookhagen, B., Glaser, P. H., and Harvey, C. F.: A unified explanation for the morphology of raised peatlands, *Nature*, 625, 79–84, <https://doi.org/10.1038/s41586-023-06807-w>, 2024.
- Cohen, A. D., Raymond, R., Ramirez, A., Morales, Z., and Ponce, F.: The Changuinola peat deposit of northwestern Panama: a tropical, back-barrier, peat(coal)-forming environment, *International Journal of Coal Geology*, 12, 157–192, [https://doi.org/10.1016/0166-5162\(89\)90050-5](https://doi.org/10.1016/0166-5162(89)90050-5), 1989.
- 725 Coll, M., Cortés, J., and Sauma, D.: Características físico-químicas y determinación de plaguicidas en el agua de la laguna de Gandoca, Limón, Costa Rica, *Revista de Biología Tropical*, 52, 33–42, 2004.
- Cortés, J.: Cahuita and Laguna Gandoca, Costa Rica, CARICOMP - Caribbean coral reef, seagrass, and mangrove sites, 107–113, 1998.



- 730 Cortés, J.: The Caribbean coastal and marine ecosystems, in: *Costa Rican Ecosystems*, University of Chicago Press, Chicago and London, 591–617, 2016.
- Couwenberg, J., Dommain, R., and Joosten, H.: Greenhouse gas fluxes from tropical peatlands in south-east Asia, *Global Change Biology*, 16, 1715–1732, <https://doi.org/10.1111/j.1365-2486.2009.02016.x>, 2010.
- 735 Crezee, B., Dargie, G. C., Ewango, C. E. N., Mitchard, E. T. A., Emba B., O., Kanyama T., J., Bola, P., Ndjango, J.-B. N., Girkin, N. T., Bocko, Y. E., Ifo, S. A., Hubau, W., Seidensticker, D., Batumike, R., Imani, G., Cuni-Sanchez, A., Kiahtipes, C. A., Lebamba, J., Wotzka, H.-P., Bean, H., Baker, T. R., Baird, A. J., Boom, A., Morris, P. J., Page, S. E., Lawson, I. T., and Lewis, S. L.: Mapping peat thickness and carbon stocks of the central Congo Basin using field data, *Nat. Geosci.*, 15, 639–644, <https://doi.org/10.1038/s41561-022-00966-7>, 2022.
- 740 Dadap, N. C., Cobb, A. R., Hoyt, A. M., Harvey, C. F., Feldman, A. F., Im, E.-S., and Konings, A. G.: Climate change-induced peatland drying in Southeast Asia, *Environ. Res. Lett.*, 17, 074026, <https://doi.org/10.1088/1748-9326/ac7969>, 2022.
- Dargie, G. C., Lewis, S. L., Lawson, I. T., Mitchard, E. T. A., Page, S. E., Bocko, Y. E., and Ifo, S. A.: Age, extent and carbon storage of the central Congo Basin peatland complex, *Nature*, 542, 86–90, <https://doi.org/10.1038/nature21048>, 2017.
- 745 Dargie, G. C., del Aguila-Pasquel, J., Córdova Oroche, C. J., Irarica Pacaya, J., Reyna Huaymacari, J., Baker, T. R., Hastie, A., Honorio Coronado, E. N., Lewis, S. L., Roucoux, K. H., Mitchard, E. T., Williams, M., Draper, F. C. H., and Lawson, I. T.: Net primary productivity and litter decomposition rates in two distinct Amazonian peatlands, *Global Change Biology*, 30, e17436, <https://doi.org/10.1111/gcb.17436>, 2024.
- Dean, W. E.: Determination of carbonate and organic matter in calcareous sediments and sedimentary rocks by loss on ignition; comparison with other methods, *Journal of Sedimentary Research*, 44, 242–248, <https://doi.org/10.1306/74D729D2-2B21-11D7-8648000102C1865D>, 1974.
- 750 Denyer, P.: Historic-prehistoric earthquakes, seismic hazards, and Tertiary and Quaternary geology of the Gandoca-Manzanillo National Wildlife Refuge, Limón, Costa Rica, *Revista de Biología Tropical*, 46, 237–250, 1998.
- Dommain, R., Couwenberg, J., Glaser, P. H., Joosten, H., and Suryadiputra, I. N. N.: Carbon storage and release in Indonesian peatlands since the last deglaciation, *Quaternary Science Reviews*, 97, 1–32, <https://doi.org/10.1016/j.quascirev.2014.05.002>, 2014.
- 755 Dommain, R., Cobb, A. R., Joosten, H., Glaser, P. H., Chua, A. F. L., Gandois, L., Kai, F.-M., Noren, A., Salim, K. A., Su'ut, N. S. H., and Harvey, C. F.: Forest dynamics and tip-up pools drive pulses of high carbon accumulation rates in a tropical peat dome in Borneo (Southeast Asia), *Journal of Geophysical Research: Biogeosciences*, 120, 617–640, <https://doi.org/10.1002/2014JG002796>, 2015.
- 760 Draper, F. C., Roucoux, K. H., Lawson, I. T., Mitchard, E. T. A., Honorio Coronado, E. N., Lähteenoja, O., Torres Montenegro, L., Valderrama Sandoval, E., Zaráte, R., and Baker, T. R.: The distribution and amount of carbon in the largest peatland complex in Amazonia, *Environ. Res. Lett.*, 9, 124017, <https://doi.org/10.1088/1748-9326/9/12/124017>, 2014.
- 765 Garcin, Y., Schefuß, E., Dargie, G. C., Hawthorne, D., Lawson, I. T., Sebag, D., Biddulph, G. E., Crezee, B., Bocko, Y. E., Ifo, S. A., Mampouya Wenina, Y. E., Mbemba, M., Ewango, C. E. N., Emba, O., Bola, P., Kanyama Tabu, J., Tyrrell, G., Young, D. M., Gassier, G., Girkin, N. T., Vane, C. H., Adatte, T., Baird, A. J., Boom, A., Gulliver, P., Morris, P. J., Page, S. E., Sjögersten, S., and Lewis, S. L.: Hydroclimatic vulnerability of peat carbon in the central Congo Basin, *Nature*, 612, 277–282, <https://doi.org/10.1038/s41586-022-05389-3>, 2022.
- Gillespie, R. and Hedges, R. E. M.: Sample Chemistry for the Oxford High Energy Mass Spectrometer, *Radiocarbon*, 25, 771–774, <https://doi.org/10.1017/S0033822200006123>, 1983.
- 770 Gillman, L. N., Wright, S. D., Cusens, J., McBride, P. D., Malhi, Y., and Whittaker, R. J.: Latitude, productivity and species richness, *Global Ecology and Biogeography*, 24, 107–117, <https://doi.org/10.1111/geb.12245>, 2015.



Girkin, N. T., Siegenthaler, A., Lopez, O., Stott, A., Ostle, N., Gauci, V., and Sjögersten, S.: Plant root carbon inputs drive methane production in tropical peatlands, *Sci Rep*, 15, 3244, <https://doi.org/10.1038/s41598-025-87467-w>, 2025.

Gorham, E.: Northern Peatlands: Role in the Carbon Cycle and Probable Responses to Climatic Warming, *Ecological Applications*, 1, <https://doi.org/10.2307/1941811>, 1991.

775 Gumbrecht, T., Roman-Cuesta, R. M., Verchot, L., Herold, M., Wittmann, F., Householder, E., Herold, N., and Murdiyarso, D.: An expert system model for mapping tropical wetlands and peatlands reveals South America as the largest contributor, *Global Change Biology*, 23, 3581–3599, <https://doi.org/10.1111/gcb.13689>, 2017.

780 Hastie, A., Honorio Coronado, E. N., Reyna, J., Mitchard, E. T. A., Åkesson, C. M., Baker, T. R., Cole, L. E. S., Oroche, C. J. C., Dargie, G., Dávila, N., De Grandi, E. C., Del Águila, J., Del Castillo Torres, D., De La Cruz Paiva, R., Draper, F. C., Flores, G., Grández, J., Hergoualc'h, K., Householder, J. E., Janovec, J. P., Läfteenoja, O., Reyna, D., Rodríguez-Veiga, P., Roucoux, K. H., Tobler, M., Wheeler, C. E., Williams, M., and Lawson, I. T.: Risks to carbon storage from land-use change revealed by peat thickness maps of Peru, *Nat. Geosci.*, 15, 369–374, <https://doi.org/10.1038/s41561-022-00923-4>, 2022.

Hedgpeth, A., Hoyt, A. M., Cavanaugh, K. C., McFarlane, K. J., and Cusack, D. F.: From the top: surface-derived carbon fuels greenhouse gas production at depth in a peatland, *Biogeosciences*, 22, 2667–2690, <https://doi.org/10.5194/bg-22-2667-2025>, 2025.

785 Heller, C., Ellerbrock, R. H., Roßkopf, N., Klingenuß, C., and Zeitz, J.: Soil organic matter characterization of temperate peatland soil with FTIR-spectroscopy: effects of mire type and drainage intensity, *European Journal of Soil Science*, 66, 847–858, <https://doi.org/10.1111/ejss.12279>, 2015.

Hergoualc'h, K. and Verchot, L. V.: Stocks and fluxes of carbon associated with land use change in Southeast Asian tropical peatlands: A review, *Global Biogeochemical Cycles*, 25, <https://doi.org/10.1029/2009GB003718>, 2011.

790 Hodgkins, S. B., Richardson, C. J., Dommain, R., Wang, H., Glaser, P. H., Verbeke, B., Winkler, B. R., Cobb, A. R., Rich, V. I., Missilmani, M., Flanagan, N., Ho, M., Hoyt, A. M., Harvey, C. F., Vining, S. R., Hough, M. A., Moore, T. R., Richard, P. J. H., De la Cruz, F. B., Toufaily, J., Hamdan, R., Cooper, W. T., and Chanton, J. P.: Tropical peatland carbon storage linked to global latitudinal trends in peat recalcitrance, *Nat. Commun.*, 9, 3640, <https://doi.org/10.1038/s41467-018-06050-2>, 2018.

795 Holmgren, A. and Nordén, B.: Characterization of Peat Samples by Diffuse Reflectance FT-IR Spectroscopy, *Appl Spectrosc*, 42, 255–262, <https://doi.org/10.1366/0003702884428284>, 1988.

Hooghiemstra, H., Cleef, A. M., Noldus, C. W., and Kappelle, M.: Upper Quaternary vegetation dynamics and palaeoclimatology of the La Chonta bog area (Cordillera de Talamanca, Costa Rica), *Journal of Quaternary Science*, 7, 205–225, <https://doi.org/10.1002/jqs.3390070303>, 1992.

800 Horn, S. P.: Timing of deglaciation in the Cordillera de Talamanca, Costa Rica, *Clim. Res.*, 1, 81–83, <https://doi.org/10.3354/cr001081>, 1990.

Hoyos-Santillan, J., Lomax, B. H., Large, D., Turner, B. L., Boom, A., Lopez, O. R., and Sjögersten, S.: Getting to the root of the problem: litter decomposition and peat formation in lowland Neotropical peatlands, *Biogeochemistry*, 126, 115–129, <https://doi.org/10.1007/s10533-015-0147-7>, 2015.

805 Hoyos-Santillan, J., Lomax, B. H., Large, D., Turner, B. L., Boom, A., Lopez, O. R., and Sjögersten, S.: Quality not quantity: Organic matter composition controls of CO<sub>2</sub> and CH<sub>4</sub> fluxes in neotropical peat profiles, *Soil Biology and Biochemistry*, 103, 86–96, <https://doi.org/10.1016/j.soilbio.2016.08.017>, 2016.

Hoyt, A. M., Chaussard, E., Seppäläinen, S. S., and Harvey, C. F.: Widespread subsidence and carbon emissions across Southeast Asian peatlands, *Nat. Geosci.*, 13, 435–440, <https://doi.org/10.1038/s41561-020-0575-4>, 2020.

810 Islebe, G. A., Hooghiemstra, H., and Borg, K. van der: The Younger Dryas climatic event in the Cordillera de Talamanca, Costa Rica (extended abstract), *Netherlands Journal of Geosciences*, 281–283, 1995.



Islebe, G. A., Hooghiemstra, H., and van 't Veer, R.: Holocene Vegetation and Water Level History in Two Bogs of the Cordillera de Talamanca, Costa Rica, *Vegetatio*, 124, 155–171, 1996.

Jiménez, J.: Bogs, Marshes, and Swamps of Costa Rica, in: *Costa Rican Ecosystems*, University of Chicago Press, Chicago and London, 683–705, 2016.

815 Jiménez, J. E.: *Guía de plantas comunes de los humedales del Área de Conservación Arenal - Huetar Norte*, Sistema Nacional de Áreas de Conservación, Costa Rica, 2018.

Joosten, H. and Clark, D.: *Wise use of mires and peatlands*, International Mire Conservation Group and International Peat Society, 2002.

820 Kaila, A.: Determination of the degree of humification in peat samples, *Agricultural and Food Science*, 28, 18–35, <https://doi.org/10.23986/afsci.71402>, 1956.

Kellerman, A. M., Kothawala, D. N., Dittmar, T., and Tranvik, L. J.: Persistence of dissolved organic matter in lakes related to its molecular characteristics, *Nature Geosci*, 8, 454–457, <https://doi.org/10.1038/ngeo2440>, 2015.

Knorr, W., Prentice, I. C., House, J. I., and Holland, E. A.: Long-term sensitivity of soil carbon turnover to warming, *Nature*, 433, 298–301, <https://doi.org/10.1038/nature03226>, 2005.

825 Krumins, J., Klavins, M., Seglins, V., and Kaup, E.: Comparative Study of Peat Composition by using FT-IR Spectroscopy, *Rigas Tehniskas Universitates Zinatniskie Raksti*, 26, 106, 2012.

Kuhry, P. and Vitt, D. H.: Fossil Carbon/Nitrogen Ratios as a Measure of Peat Decomposition, *Ecology*, 77, 271–275, <https://doi.org/10.2307/2265676>, 1996.

830 Kutterolf, S., Brenner, M., Dull, R. A., Freundt, A., Kallmeyer, J., Krastel, S., Katsev, S., Lebas, E., Meyer, A., Pérez, L., Rausch, J., Saballos, A., Schwalb, A., and Strauch, W.: Workshop on drilling the Nicaraguan lakes: bridging continents and oceans (NICA-BRIDGE), *Scientific Drilling*, 32, 73–84, <https://doi.org/10.5194/sd-32-73-2023>, 2023.

Lähteenoja, O. and Page, S.: High diversity of tropical peatland ecosystem types in the Pastaza-Marañón basin, Peruvian Amazonia, *Journal of Geophysical Research: Biogeosciences*, 116, <https://doi.org/10.1029/2010JG001508>, 2011.

835 Lähteenoja, O., Ruokolainen, K., Schulman, L., and Oinonen, M.: Amazonian peatlands: an ignored C sink and potential source, *Global Change Biology*, 15, 2311–2320, <https://doi.org/10.1111/j.1365-2486.2009.01920.x>, 2009.

Lähteenoja, O., Reátegui, Y. R., Räsänen, M., Torres, D. D. C., Oinonen, M., and Page, S.: The large Amazonian peatland carbon sink in the subsiding Pastaza-Marañón foreland basin, Peru, *Global Change Biology*, 18, 164–178, <https://doi.org/10.1111/j.1365-2486.2011.02504.x>, 2012.

840 Lähteenoja, O., Flores, B., and Nelson, B.: Tropical Peat Accumulation in Central Amazonia, *Wetlands*, 33, 495–503, <https://doi.org/10.1007/s13157-013-0406-0>, 2013.

Lawson, I. T., Jones, T. D., Kelly, T. J., Coronado, E. N. H., and Roucoux, K. H.: The Geochemistry of Amazonian Peats, *Wetlands*, 34, 905–915, <https://doi.org/10.1007/s13157-014-0552-z>, 2014.

845 Lawson, I. T., Åkesson, C. M., Dargie, G. C., del Aguila Pasquel, J., Draper, F. C., Hastie, A., Kelly, T. J., Sassoon, D., Abraham, V., Baker, T. R., Fabel, D., Gulliver, P., Honorio Coronado, E. N., and Roucoux, K. H.: Holocene patterns of peat accumulation in Peruvian Amazonia, *Palaeogeography, Palaeoclimatology, Palaeoecology*, 686, 113579, <https://doi.org/10.1016/j.palaeo.2026.113579>, 2026.

Legendre, P. and Anderson, M. J.: Distance-Based Redundancy Analysis: Testing Multispecies Responses in Multifactorial Ecological Experiments, *Ecological Monographs*, 69, 1–24, [https://doi.org/10.1890/0012-9615\(1999\)069%255B0001:DBRATM%255D2.0.CO;2](https://doi.org/10.1890/0012-9615(1999)069%255B0001:DBRATM%255D2.0.CO;2), 1999.



- 850 Leifeld, J. and Menichetti, L.: The underappreciated potential of peatlands in global climate change mitigation strategies, *Nat Commun*, 9, 1071, <https://doi.org/10.1038/s41467-018-03406-6>, 2018.
- Leri, A. C., Loisel, J., Parke, I., Pavia, A. P., Ravel, B., Northrup, P., and Liu, Y.: Long-term peat organic matter stability influenced by botanical composition and oceanic bromide inputs, *Geoderma*, 464, 117633, <https://doi.org/10.1016/j.geoderma.2025.117633>, 2025.
- 855 Liu, X., Xiong, Y., and Liao, B.: Relative contributions of leaf litter and fine roots to soil organic matter accumulation in mangrove forests, *Plant and Soil*, 421, 1–11, <https://doi.org/10.1007/s11104-017-3477-5>, 2017.
- Loisel, J. and Yu, Z.: Holocene peatland carbon dynamics in Patagonia, *Quaternary Science Reviews*, 69, 125–141, <https://doi.org/10.1016/j.quascirev.2013.02.023>, 2013.
- 860 Loisel, J., Garneau, M., and Hélie, J.-F.: Modern Sphagnum  $\delta^{13}\text{C}$  signatures follow a surface moisture gradient in two boreal peat bogs, James Bay lowlands, Québec, *Journal of Quaternary Science*, 24, 209–214, <https://doi.org/10.1002/jqs.1221>, 2009.
- Loisel, J., Yu, Z., Beilman, D., Camill, P., Alm, J., Amesbury, M., Anderson, D., Andersson, S., Bochicchio, C., Barber, K., Belyea, L., Bunbury, J., Chambers, F., Charman, D., Vleeschouwer, F., Fiałkiewicz-koziół, B., Finkelstein, S., Gafka, M., Garneau, M., and Zhou, W.: A database and synthesis of northern peatland soil properties and Holocene carbon and nitrogen accumulation, *The Holocene*, 24, <https://doi.org/10.1177/0959683614538073>, 2014.
- 865 Loisel, J., Peters, J., Tegetmeyer, C., Girkin, N., Parsekian, A., and Rivera Wong, J.: Observations from an expedition to Costa Rican peatlands, *The Society of Wetland Scientists*, 42, 145–149, 2024.
- Lourenco, M., Fitchett, J. M., and Woodborne, S.: Peat definitions: A critical review, *Progress in Physical Geography: Earth and Environment*, 47, 506–520, <https://doi.org/10.1177/03091333221118353>, 2023.
- 870 Malmer, N. and Holm, E.: Variation in the C/N-Quotient of Peat in Relation to Decomposition Rate and Age Determination with  $^{210}\text{Pb}$ , *Oikos*, 43, 171–182, <https://doi.org/10.2307/3544766>, 1984.
- Martínez Cortizas, A., López-Merino, L., Silva-Sánchez, N., Sjöström, J. K., and Kylander, M. E.: Investigating the Mineral Composition of Peat by Combining FTIR-ATR and Multivariate Analysis, *Minerals*, 11, 1084, <https://doi.org/10.3390/min11101084>, 2021.
- 875 Mauquoy, D., Engelkes, T., Groot, M. H. M., Markesteijn, F., Oudejans, M. G., van der Plicht, J., and van Geel, B.: High-resolution records of late-Holocene climate change and carbon accumulation in two north-west European ombrotrophic peat bogs, *Palaeogeography, Palaeoclimatology, Palaeoecology*, 186, 275–310, [https://doi.org/10.1016/S0031-0182\(02\)00513-8](https://doi.org/10.1016/S0031-0182(02)00513-8), 2002.
- Mauquoy, D., Hughes, P., and Geel, B.: A protocol for plant macrofossil analysis of peat deposits, *Mires and Peat*, 7, 1–5, 2010.
- McCloskey, T. and Liu, K.: A sedimentary-based history of hurricane strikes on the southern Caribbean coast of Nicaragua, *Quaternary Research*, 78, 454–464, <https://doi.org/10.1016/j.yqres.2012.07.003>, 2012.
- 880 McKee, K., Cahoon, D., and Feller, I.: Caribbean mangroves adjust to rising sea level through biotic controls on soil elevation change, *Global Ecology and Biogeography*, 16, 545–556, <https://doi.org/10.1111/j.1466-8238.2007.00317.x>, 2007.
- Meentemeyer, V.: Macroclimate and Lignin Control of Litter Decomposition Rates, *Ecology*, 59, 465–472, <https://doi.org/10.2307/1936576>, 1978.
- 885 Melton, J. R., Chan, E., Millard, K., Fortier, M., Winton, R. S., Martín-López, J. M., Cadillo-Quiroz, H., Kidd, D., and Verchot, L. V.: A map of global peatland extent created using machine learning (Peat-ML), *Geoscientific Model Development*, 15, 4709–4738, <https://doi.org/10.5194/gmd-15-4709-2022>, 2022.
- Middleton, B. A. and McKee, K. L.: Degradation of Mangrove Tissues and Implications for Peat Formation in Belizean Island Forests, *Journal of Ecology*, 89, 818–828, 2001.



- 890 Moreno-Casasola, P. and Warner, B. G.: Breviario para describir, observar y manejar humedales, 1. ed., RAMSAR, Xalapa, Veracruz, México, 2009.
- Müller, C. M., Pejcic, B., Esteban, L., Piane, C. D., Raven, M., and Mizaikoff, B.: Infrared Attenuated Total Reflectance Spectroscopy: An Innovative Strategy for Analyzing Mineral Components in Energy Relevant Systems, *Sci Rep*, 4, 6764, <https://doi.org/10.1038/srep06764>, 2014.
- 895 Norris, M. W., Turnbull, J. C., Howarth, J. D., and Vandergoes, M. J.: Pretreatment of Terrestrial Macrofossils, *Radiocarbon*, 62, 349–360, <https://doi.org/10.1017/RDC.2020.8>, 2020.
- Obando, L. and Malavassi, L.: Geology of peat deposits of Costa Rica, *Revista Geológica de América Central*, <https://doi.org/10.15517/rgac.v0i15.13233>, 1993.
- Obando, L. Gmo., Malavassi, L. R., and Estrada, R.: Deposits of Peat in Costa Rica, in: *Energy and Mineral Potential of the Central American-Caribbean Region*, edited by: Miller, R. L., Escalante, G., Reinemund, J. A., and Bergin, M. J., Springer, Berlin, Heidelberg, 199–207, [https://doi.org/10.1007/978-3-642-79476-6\\_27](https://doi.org/10.1007/978-3-642-79476-6_27), 1995.
- 900 Oksanen, J., Simpson, G. L., Blanchet, F. G., Kindt, R., Legendre, P., Minchin, P. R., O'Hara, R. B., Solymos, P., Stevens, M. H. H., Szoecs, E., Wagner, H., Barbour, M., Bedward, M., Bolker, B., Borcard, D., Borman, T., Carvalho, G., Chirico, M., Cáceres, M. D., Durand, S., Evangelista, H. B. A., FitzJohn, R., Friendly, M., Furneaux, B., Hannigan, G., Hill, M. O., Lahti, L., Martino, C., McGlinn, D., Ouellette, M.-H., Cunha, E. R., Smith, T., Stier, A., Braak, C. J. F. T., and Weedon, J.: *vegan: Community Ecology Package*, 2025.
- 905 Page, S., Rieley, J. O., and Banks, C. J.: Global and regional importance of the tropical peatland carbon pool, *Global Change Biology*, 17, 798–818, <https://doi.org/10.1111/j.1365-2486.2010.02279.x>, 2011.
- Pérez-Castillo, A. G., Monge-Muñoz, M., Durán-Quesada, A. M., Giraldo-Sanclemente, W., Méndez-Esquivel, A. C., Briceño-Soto, N., and Cadillo-Quiroz, H.: Vegetation and Peat Soil Characteristics of a Fire-Impacted Tropical Peatland in Costa Rica, *Wetlands*, 44, <https://doi.org/10.1007/s13157-024-01797-5>, 2024.
- 910 Peters, J. and Tegetmeyer, C.: Inventory of peatlands in the Caribbean and first description of priority areas, *Proceedings of the Griefswald Mire Centre*, 2019.
- Phillips, S.: Hologene evolution of the changuinola peat deposit, Panama: sedimentology of a marine-influenced tropical peat deposit on a tectonically active coast, University of British Columbia, <https://doi.org/10.14288/1.0052918>, 1995.
- 915 Phillips, S. and Bustin, R. M.: Sedimentology of the Changuinola peat deposit: Organic and clastic sedimentary response to punctuated coastal subsidence, *Geological Society of America Bulletin*, 108, 794–814, [https://doi.org/10.1130/0016-7606\(1996\)108%253C0794:SOTCPD%253E2.3.CO;2](https://doi.org/10.1130/0016-7606(1996)108%253C0794:SOTCPD%253E2.3.CO;2), 1996.
- Phillips, S., Rouse, G. E., and Bustin, R. M.: Vegetation zones and diagnostic pollen profiles of a coastal peat swamp, Bocas del Toro, Panamá, *Palaeogeography, Palaeoclimatology, Palaeoecology*, 128, 301–338, [https://doi.org/10.1016/S0031-0182\(97\)81129-7](https://doi.org/10.1016/S0031-0182(97)81129-7), 1997.
- 920 R Core Team: *R: A Language and Environment for Statistical Computing*, R Foundation for Statistical Computing, Vienna, Austria, 2024.
- Rabel, E. and Loisel, J.: The spatial distribution and paleoecology of Caribbean peatlands, *Commun Earth Environ*, 5, 1–11, <https://doi.org/10.1038/s43247-024-01903-9>, 2024.
- 925 Rabel, E., Loisel, J., Barthelmes, A., Malpica-Piñeros, C., Tegetmeyer, C., Wong, J. R., and Villegas-Mejía, L.: A probabilistic map of Costa Rican peatlands based on vegetation, ecosystem, and soil inventories, *Sci Rep*, 15, 18088, <https://doi.org/10.1038/s41598-025-03126-0>, 2025.
- Ramsar: The List of Wetlands of International Importance, The Convention on Wetlands, <https://www.ramsar.org/sites/default/files/2023-08/sitelist.pdf>, 2026.



- 930 Reig, F. B., Adelantado, J. V. G., and Moya Moreno, M. C. M.: FTIR quantitative analysis of calcium carbonate (calcite) and silica (quartz) mixtures using the constant ratio method. Application to geological samples, *Talanta*, 58, 811–821, [https://doi.org/10.1016/S0039-9140\(02\)00372-7](https://doi.org/10.1016/S0039-9140(02)00372-7), 2002.
- Reimer, P. J., Austin, W. E. N., Bard, E., Bayliss, A., Blackwell, P. G., Ramsey, C. B., Butzin, M., Cheng, H., Edwards, R. L., Friedrich, M., Grootes, P. M., Guilderson, T. P., Hajdas, I., Heaton, T. J., Hogg, A. G., Hughen, K. A., Kromer, B., Manning, S. W., Muscheler, R., Palmer, J. G., Pearson, C., Plicht, J. van der, Reimer, R. W., Richards, D. A., Scott, E. M., Southon, J. R., Turney, C. S. M., Wacker, L., Adolphi, F., Büntgen, U., Capano, M., Fahrni, S. M., Fogtmann-Schulz, A., Friedrich, R., Köhler, P., Kudsk, S., Miyake, F., Olsen, J., Reinig, F., Sakamoto, M., Sookdeo, A., and Talamo, S.: The IntCal20 Northern Hemisphere Radiocarbon Age Calibration Curve (0–55 cal kBP), *Radiocarbon*, 62, 725–757, <https://doi.org/10.1017/RDC.2020.41>, 2020.
- 935
- Ribeiro, K., Pacheco, F. S., Ferreira, J. W., de Sousa-Neto, E. R., Hastie, A., Krieger Filho, G. C., Alvalá, P. C., Forti, M. C., and Ometto, J. P.: Tropical peatlands and their contribution to the global carbon cycle and climate change, *Global Change Biology*, 27, 489–505, <https://doi.org/10.1111/gcb.15408>, 2021.
- 940
- Rizzo, M. and Szekely, G.: energy: E-Statistics: Multivariate Inference via the Energy of Data, 2024.
- Rodgers, J. C. and Horn, S. P.: Modern pollen spectra from Costa Rica, *Palaeogeography, Palaeoclimatology, Palaeoecology*, 124, 53–71, [https://doi.org/10.1016/0031-0182\(96\)00004-1](https://doi.org/10.1016/0031-0182(96)00004-1), 1996.
- 945
- Roucoux, K. H., Lawson, I. T., Jones, T. D., Baker, T. R., Coronado, E. N. H., Gosling, W. D., and Läähteenoja, O.: Vegetation development in an Amazonian peatland, *Palaeogeography, Palaeoclimatology, Palaeoecology*, 374, 242–255, <https://doi.org/10.1016/j.palaeo.2013.01.023>, 2013.
- Rovai, A. S., Twilley, R. R., Castañeda-Moya, E., Riul, P., Cifuentes-Jara, M., Manrow-Villalobos, M., Horta, P. A., Simonassi, J. C., Fonseca, A. L., and Pagliosa, P. R.: Global controls on carbon storage in mangrove soils, *Nature Clim Change*, 8, 534–538, <https://doi.org/10.1038/s41558-018-0162-5>, 2018.
- 950
- Ruwaimana, M., Anshari, G. Z., Silva, L. C. R., and Gavin, D. G.: The oldest extant tropical peatland in the world: a major carbon reservoir for at least 47 000 years, *Environ. Res. Lett.*, 15, 114027, <https://doi.org/10.1088/1748-9326/abb853>, 2020.
- Rydin, H. and Jeglum, J. K.: Peat and organic soil, in: *The Biology of Peatlands*, edited by: Rydin, H. and Jeglum, J. K., Oxford University Press, 85–108, <https://doi.org/10.1093/acprof:osobl/9780199602995.003.0005>, 2013.
- 955
- Sasmito, S. D., Taillardat, P., Adinugroho, W. C., Krisnawati, H., Novita, N., Fatoyinbo, L., Friess, D. A., Page, S. E., Lovelock, C. E., Murdiyoso, D., Taylor, D., and Lupascu, M.: Half of land use carbon emissions in Southeast Asia can be mitigated through peat swamp forest and mangrove conservation and restoration, *Nat Commun*, 16, 740, <https://doi.org/10.1038/s41467-025-55892-0>, 2025.
- 960
- Sciumbata, M., Wenina, Y. E. M., Mbemba, M., Dargie, G. C., Baird, A. J., Morris, P. J., Ifo, S. A., Aerts, R., and Lewis, S. L.: First estimates of fine root production in tropical peat swamp and terra firme forests of the central Congo Basin, *Sci Rep*, 13, 12315, <https://doi.org/10.1038/s41598-023-38409-x>, 2023.
- Seaton, N., Chawchai, S., Pienpinijtham, P., and Löwemark, L.: A new mangrove core record for Eastern Thailand: chemical characterization of bulk organic sediment by FTIR–ATR spectroscopy and elemental analysis, *Bulletin of Earth Sciences of Thailand*, 16, 2024.
- 965
- Sengyang, P., Rangsriwatananon, K., and Chaisena, A.: Preparation of zeolite N from metakaolinite by hydrothermal method, *Journal of Ceramic Processing Research*, 16, 111–116, 2015.
- SINAC: Proyecto Humedales de SINAC-PNUD-GEF, *Inventario Nacional De Humedales*, 12–29, 2018.
- Sjögersten, S., Siegenthaler, A., Lopez, O. R., Aplin, P., Turner, B., and Gauci, V.: Methane emissions from tree stems in neotropical peatlands, *New Phytologist*, 225, 769–781, <https://doi.org/10.1111/nph.16178>, 2020.



- 970 Slate, J. E., Johnson, T. C., and Moore, T. C.: Impact of pre-Columbian agriculture, climate change, and tectonic activity inferred from a 5,700-year paleolimnological record from Lake Nicaragua, *J Paleolimnol*, 50, 139–149, <https://doi.org/10.1007/s10933-013-9709-7>, 2013.
- Stanek, W. and Silc, T.: Comparisons of four methods for determination of degree of peat humification (decomposition) with emphasis on the Von Post method, *Can. J. Soil. Sci.*, 57, 109–117, <https://doi.org/10.4141/cjss77-015>, 1977.
- 975 Stuiver, M. and Reimer, P. J.: Extended 14C Data Base and Revised CALIB 3.0 14C Age Calibration Program, *Radiocarbon*, 35, 215–230, <https://doi.org/10.1017/S0033822200013904>, 1993.
- Swindles, G. T., Whitney, B. S., Gałka, M., Mullan, D. J., Low, R., Gallego-Sala, A., Lopez, R. O., Kilbride, E., Graham, C., and Baird, A. J.: Ecohydrological Response of a Tropical Peatland to Rainfall Changes Driven by Intertropical Convergence Zone Variability, *Journal of Biogeography*, 52, 621–628, <https://doi.org/10.1111/jbi.15051>, 2024.
- 980 Tfaily, M. M., Cooper, W. T., Kostka, J. E., Chanton, P. R., Schadt, C. W., Hanson, P. J., Iversen, C. M., and Chanton, J. P.: Organic matter transformation in the peat column at Marcell Experimental Forest: Humification and vertical stratification, *Journal of Geophysical Research: Biogeosciences*, 119, 661–675, <https://doi.org/10.1002/2013JG002492>, 2014.
- Thayer, G., Oldemar, R. E., and Ramirez, A.: Economics of Selected Energy Applications of Peat in Panama and Costa Rica, in: *Energy and Mineral Potential of the Central American-Caribbean Region*, edited by: Miller, R. L., Escalante, G., Reinemund, J. A., and Bergin, M. J., Springer, Berlin, Heidelberg, 209–212, [https://doi.org/10.1007/978-3-642-79476-6\\_28](https://doi.org/10.1007/978-3-642-79476-6_28), 1995.
- 985 Thomas, Z. A., Cadd, H., Turney, C., Becerra-Valdivia, L., Haines, H. A., Marjo, C., Fogwill, C., Carter, S., and Brickle, P.: Westerly wind shifts drove Southern Hemisphere mid-latitude peat growth since the last glacial, *Nat. Geosci.*, 1–7, <https://doi.org/10.1038/s41561-025-01842-w>, 2025.
- Tian, W., Wang, H., Xiang, X., Wang, R., and Xu, Y.: Structural Variations of Bacterial Community Driven by Sphagnum Microhabitat Differentiation in a Subalpine Peatland, *Front. Microbiol.*, 10, <https://doi.org/10.3389/fmicb.2019.01661>, 2019.
- 990 Uhelski, D. M., Kane, E. S., and Chimner, R. A.: Plant functional types drive Peat Quality differences, *Wetlands*, 42, 51, <https://doi.org/10.1007/s13157-022-01572-4>, 2022.
- UNEP: *Global Peatlands Assessment: The State of the World's Peatlands*, 2022.
- Upton, A., Vane, C. H., Girkin, N., Turner, B. L., and Sjögersten, S.: Does litter input determine carbon storage and peat organic chemistry in tropical peatlands?, *Geoderma*, 326, 76–87, <https://doi.org/10.1016/j.geoderma.2018.03.030>, 2018.
- 995 Urquhart, G. R.: Paleoecological record of hurricane disturbance and forest regeneration in Nicaragua, *Quaternary International*, 195, 88–97, <https://doi.org/10.1016/j.quaint.2008.05.012>, 2009.
- Urrego, L. E., Prado, M. A., Bernal, G., and Galeano, A.: Mangrove responses to droughts since the little ice age in the Colombian Caribbean, *Estuarine, Coastal and Shelf Science*, 230, 106432, <https://doi.org/10.1016/j.ecss.2019.106432>, 2019.
- 1000 Verbeke, B. A., Lamit, L. J., Lilleskov, E. A., Hodgkins, S. B., Basiliko, N., Kane, E. S., Andersen, R., Artz, R. R. E., Benavides, J. C., Benschoter, B. W., Borken, W., Bragazza, L., Brandt, S. M., Bräuer, S. L., Carson, M. A., Charman, D., Chen, X., Clarkson, B. R., Cobb, A. R., Convey, P., Pasquel, J. del Á., Enriquez, A. S., Griffiths, H., Grover, S. P., Harvey, C. F., Harris, L. I., Hazard, C., Hodgson, D., Hoyt, A. M., Hribljan, J., Jauhiainen, J., Juutinen, S., Knorr, K.-H., Kolka, R. K., Könönen, M., Larmola, T., McCalley, C. K., McLaughlin, J., Moore, T. R., Mykityczuk, N., Normand, A. E., Rich, V., Roulet, N., Royles, J., Rutherford, J., Smith, D. S., Svenning, M. M., Tedersoo, L., Thu, P. Q., Trettin, C. C., Tuittila, E.-S., Urbanová, Z., Varner, R. K., Wang, M., Wang, Z., Warren, M., Wiedermann, M. M., Williams, S., Yavitt, J. B., Yu, Z.-G., Yu, Z., and Chanton, J. P.: Latitude, Elevation, and Mean Annual Temperature Predict Peat Organic Matter Chemistry at a Global Scale, *Global Biogeochemical Cycles*, 36, e2021GB007057, <https://doi.org/10.1029/2021GB007057>, 2022.
- 1005 Villegas-Mejía, L.: *Mapping of Coastal Peatlands in the Caribbean Region: Colombia and Costa Rica*, Institute of Botany and Landscape Ecology, University of Griefswald, 2018.
- 1010



- Wang, Y.-H., Zhang, P., He, C., Yu, J.-C., Shi, Q., Dahlgren, R. A., Spencer, R. G. M., Yang, Z.-B., and Wang, J.-J.: Molecular signatures of soil-derived dissolved organic matter constrained by mineral weathering, *Fundam Res*, 3, 377–383, <https://doi.org/10.1016/j.fmre.2022.01.032>, 2022.
- Wei, T. and Simko, V.: R package “corrplot”: Visualization of a Correlation Matrix, 2024.
- 1015 Wickham, H.: *ggplot2: Elegant Graphics for Data Analysis*, Springer-Verlag New York, 2016.
- Wickham, H., François, R., Henry, L., Müller, K., and Vaughan, D.: *dplyr: A Grammar of Data Manipulation*, 2023.
- Winton, R. S., Benavides, J. C., Mendoza, E., Uhde, A., Hastie, A., Honorio Coronado, E. N., Hernandez Ortega, A. G., Pauku, S., Mullins, B., del Aguila Pasquel, J., Aymard-Corredor, G. A., Baker, T. R., Draper, F. C., Flores Llampazo, G., Herrera, R., Phillips, O. L., Reyna Huaymacari, J. M., ter Steege, H., Stropp, J., Lawson, I. T., Gallego-Sala, A. V., Boom, A., Wehrli, B., and Hoyt, A. M.: Widespread carbon-dense peatlands in the Colombian lowlands, *Environ. Res. Lett.*, 20, 054025, <https://doi.org/10.1088/1748-9326/adbc03>, 2025.
- 1020 Wright, E. L., Black, C. R., Cheesman, A. W., Turner, B. L., and Sjögersten, S.: Impact of Simulated Changes in Water Table Depth on Ex Situ Decomposition of Leaf Litter from a Neotropical Peatland, *Wetlands*, 33, 217–226, <https://doi.org/10.1007/s13157-012-0369-6>, 2013.
- 1025 Xiong, Y., Liu, X., Guan, W., Liao, B., Chen, Y., Li, M., and Zhong, C.: Fine root functional group based estimates of fine root production and turnover rate in natural mangrove forests, *Plant and Soil*, 413, <https://doi.org/10.1007/s11104-016-3082-z>, 2017.
- Xu, J., Morris, P. J., Liu, J., and Holden, J.: PEATMAP: Refining estimates of global peatland distribution based on a meta-analysis, *CATENA*, 160, 134–140, <https://doi.org/10.1016/j.catena.2017.09.010>, 2018.
- 1030 Young, D. M., Baird, A. J., Morris, P. J., Dargie, G. C., Mampouya Wenina, Y. E., Mbemba, M., Boom, A., Cook, P., Betts, R., Burke, E., Bocko, Y. E., Chadburn, S., Crabtree, D. E., Crezee, B., Ewango, C. E. N., Garcin, Y., Georgiou, S., Girkin, N. T., Gulliver, P., Hawthorne, D., Ifo, S. A., Lawson, I. T., Page, S. E., Jovani-Sancho, A. J., Schefuß, E., Sciumbata, M., Sjögersten, S., and Lewis, S. L.: Simulating carbon accumulation and loss in the central Congo peatlands, *Global Change Biology*, 29, 6812–6827, <https://doi.org/10.1111/gcb.16966>, 2023.
- 1035 Yu, Z., Loisel, J., Brosseau, D. P., Beilman, D. W., and Hunt, S. J.: Global peatland dynamics since the Last Glacial Maximum, *Geophysical Research Letters*, 37, <https://doi.org/10.1029/2010GL043584>, 2010.
- Yu, Z., Beilman, D. W., and Loisel, J.: Transformations of landscape and peat-forming ecosystems in response to late Holocene climate change in the western Antarctic Peninsula, *Geophysical Research Letters*, 43, 7186–7195, <https://doi.org/10.1002/2016GL069380>, 2016.
- 1040 Zar, J. H.: Spearman Rank Correlation, in: *Encyclopedia of Biostatistics*, John Wiley & Sons, Ltd, <https://doi.org/10.1002/0470011815.b2a15150>, 2005.